Batteries & Supercaps

Review
doi.org/10.1002/batt.202200502

Chemistry Europe
European Chemical Societies Publishing

www.batteries-supercaps.org

VIP *Very Important Paper*

A Review of Polymer-based Solid-State Electrolytes for Lithium-Metal Batteries: Structure, Kinetic, Interface Stability, and Application

Xiaoxue Zhao,[a] Chao Wang,[a] Hong Liu,[a] Yuhao Liang,[a] and Li-Zhen Fan*[a]

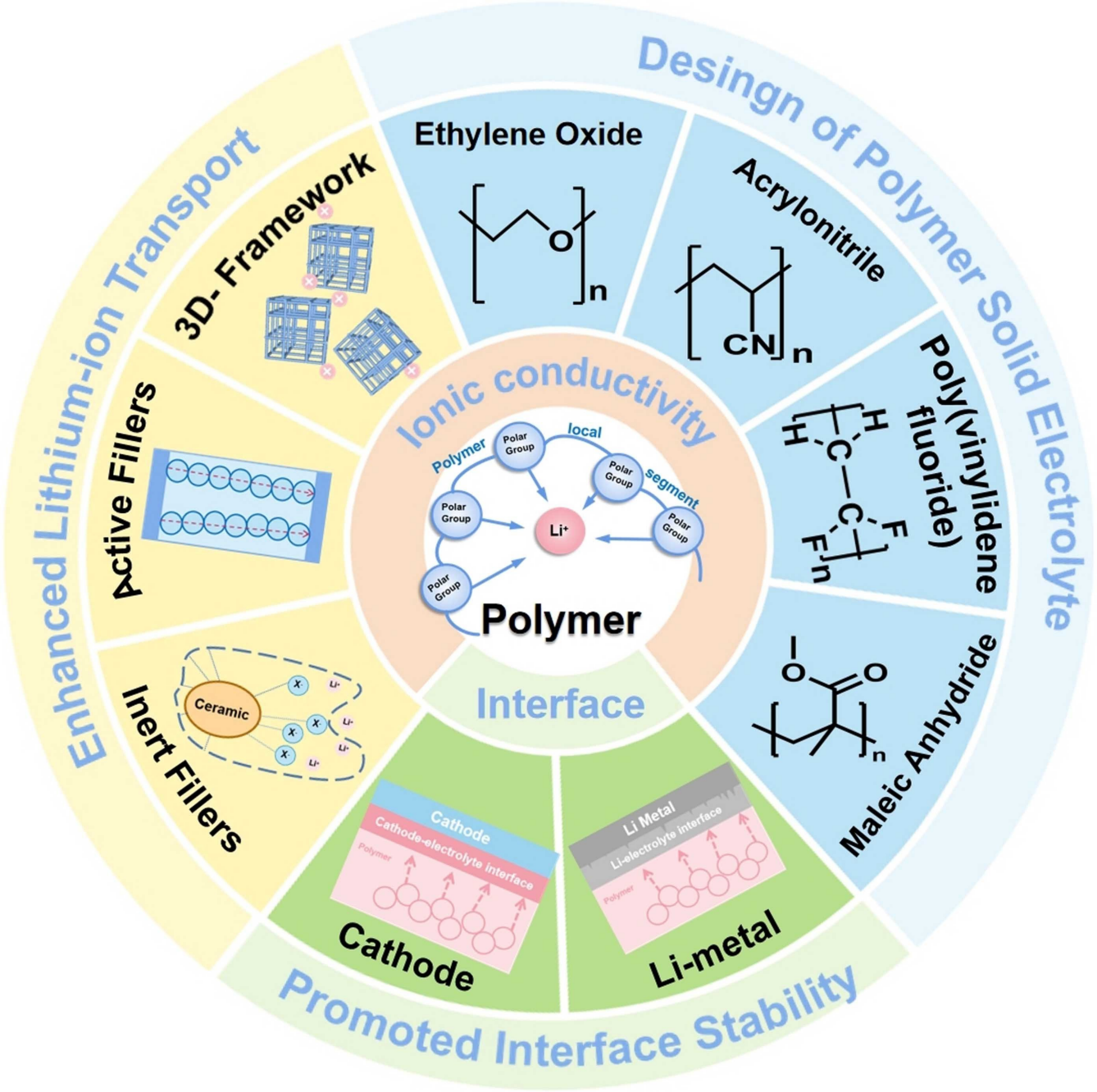

Solid-state polymer electrolytes (SPEs) for all-solid-state batteries (ASSBs) have received considerable attention owing to excellent processability, good flexibility, high safety levels, and superior thermal stability. However, the practical application of SPEs is currently restricted by their low ionic conductivity, narrow electrochemical oxidation window, and poor long-term stability of lithium (Li) metal. These challenges are mainly related to the polymer molecular structures, the dynamic of the polymer electrolyte, and the polymer compound stability at the electrode-electrolyte interface. In this review, we provide recent strategies and discuss strategies of interest for applications to high-energy-density ASSB, particularly the molecular design, ion-transport dynamic mechanisms of solid polymer electrolytes, and organic-inorganic composite. Based on recent work, perspectives on future research directions are discussed for developing solid polymer electrolytes.

1. Introduction

Energy storage devices with higher energy and power density, safety, long cycle life, and low cost have attracted extensive attention to achieve the ambitious goal of "carbon neutrality" by 2060.[1–3] Due to its high theoretical specific capacity (3860 mAh g^{-1}), and lower redox voltage (−3.04 V vs. H), lithium-metal battery has been considered as the most promising candidate for high-energy battery systems, including lithium-metal batteries,[4] lithium-sulfur battery,[5] and lithium-O_2 battery.[6] Due to uneven lithium ion deposition, the dendrites could gradually emerge at the lithium metal anode surface, triggering some issues such as local overheating, thermal runaway, and even explosion, especially in the organic carbonates liquid electrolytes.[7] Solid-state electrolyte (SSE) films can avoid combustion and organic liquid leakage, they also can adopt a multi-layer stacking process to further improve the energy density. Therefore, the SSE could be one of the most promising candidates for next-generation electrolyte materials to replace carbonate liquid electrolytes.

As a key component of all-solid-state lithium metal batteries, SSEs have drawn worldwide attention and impressive breakthroughs were made. Generally, SSEs can be mainly classified into three categories: solid-state polymer electrolytes (SPEs), solid inorganic electrolytes (SIEs), and solid composite electrolytes.[8] Specifically, compared to single-phase SIEs, SPEs are a uniform mixture composed of polymer matrix and lithium salts, which consequently possess good interface contact with the electrode, good flexibility, and excellent processability, it is currently considered to be the most promising SSE. However, the practical application of SPEs is currently restricted by their low ionic conductivity, narrow electrochemical window, and poor lithium metal stability.[9–11] Considering the advantages of polymer material, SPEs may still need further investigation.

In this review, the polymer-based SSEs used in lithium batteries will be focused on, as shown in Figure 1. Initially, we summarize the progress and challenges of polymer-based SSEs according to their molecular structures. The chemical dynamic mechanisms on ionic conductivity, and the electrochemical window will be introduced. Then we present the recently inorganic-polymer composite strategies to improve interface compatibility including lithium metal anodes and high-voltage cathodes, followed by a discussion of the current reports on the enhancement of fast ion transport. Finally, we consider issues associated with all-solid-state batteries (ASSBs), including industrialization and recycling, machine learning, as well as simulation technology. A general conclusion and perspectives on the current limitations are recommended and future research directions for polymer-based SSEs are presented.

2. Fundamentals of Polymer Materials for Solid-State Electrolytes

SPEs consist of polymer matrices, lithium salts, and additives. An ideal polymer-based electrolyte usually has the following advantages: 1) Salt dissociation: an interaction between the polymer and the cation, with the advantage of impelling ions to leap between different sites; a high dielectric constant promotes dissociation of the lithium salt and increases the charge carrier concentration; a highly flexible backbone lowers the energy barrier for bond rotation and promotes block motion of the polymer chain.[12] 2) Functional groups: molecular design allows functional groups to meet the needs of different SPEs applications.[13] 3) Physical properties: easy film manufacture, good elasticity, light weight. 4) Safety: suppression of dendrites and thermal runaways.[14,15] Here, several polymer electrolyte materials, such as polyethylene oxide (PEO),[16] polyacrylonitrile (PAN),[17] polyvinylidene fluoride (PVDF),[18] and poly(maleic anhydride) (PMMA),[19] were selected to elaborate the connection between electrolyte structures and intrinsic properties. Meanwhile, the corresponding optimization strategies for SPEs with different structures were systematically summarized to boost their application in ASSBs (Table 1).

2.1. Poly(ethylene oxide)-based polymer electrolytes

PEO is the most widely selected polymer electrolyte material due to its stable interface with a lithium anode, low cost, and high ionic conductivity compared with other polymers, the chemical molecular called H–(O–CH_2–CH_2)$_n$–OH.[20,21] In PEO

[a] X. Zhao, C. Wang, H. Liu, Y. Liang, Prof. Dr. L.-Z. Fan
Beijing Advanced Innovation Center for Materials Genome Engineering
Beijing Key Laboratory for Advanced Energy Materials and Technologies,
University of Science and Technology Beijing, Beijing 100083, China
E-mail: fanlizhen@ustb.edu.cn

This publication is part of a joint Special Collection on Solid State Batteries, featuring contributions published in Advanced Energy Materials, Energy Technology, Batteries & Supercaps, ChemSusChem, and Advanced Energy and Sustainability Research.

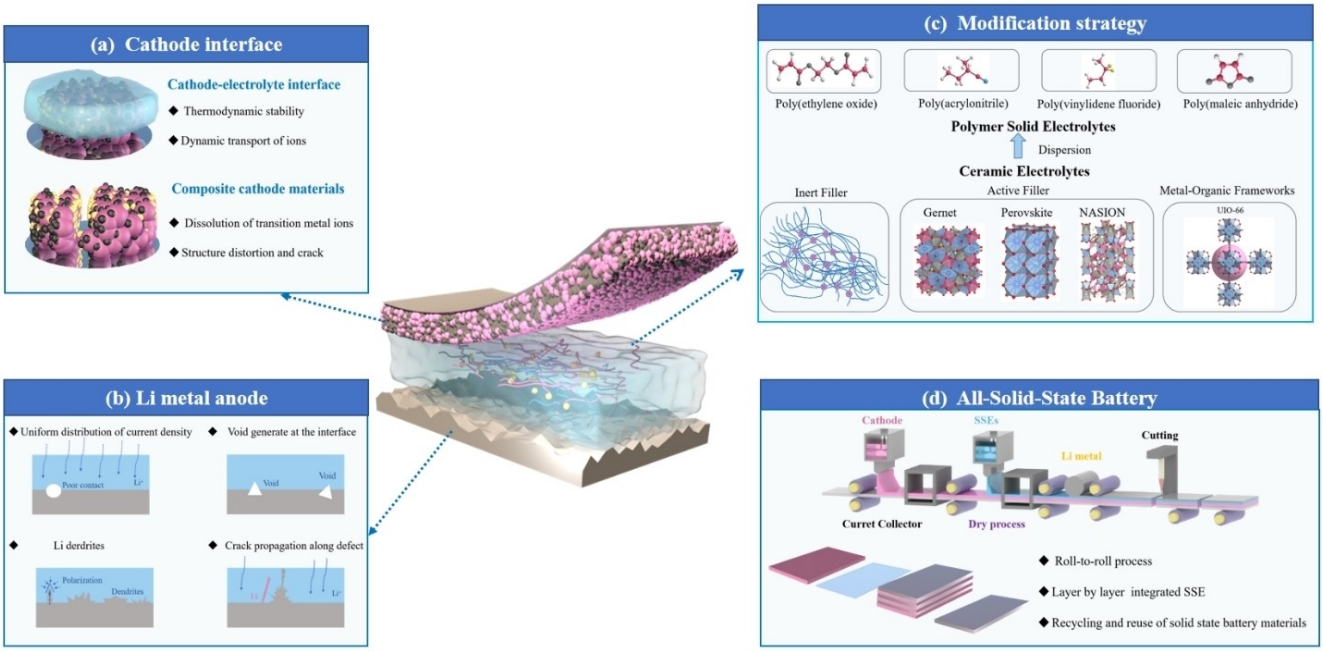

Figure 1. Schematic illustration of polymer-based electrolyte and ASSLBs industrialization.

Table 1. Summary of polymer-based solid-state electrolytes.

Electrolyte composition	Functional group	Ionic conductivity [S cm^{-1}]	Cycle performance	Voltage Window [V]	Ref.
PEO/LLZO–FEC–SN–LiTFSI	EO	1.6×10^{-4}, 25 °C	0.25 mA cm^{-2}, 600 h, 50 °C	3.9	[21]
PAN–PEO–LiTFSI	CN	$\sim10^{-4}$, 60 °C	0.30 mA cm^{-2}, 600 h, 60 °C	3.7	[76]
PVDF–$LiNSO_2$(LiTFSI)	PVDF	1.3×10^{-4}, 25 °C	0.50 mA cm^{-2}, 100 h, 25 °C	4.8	[62]
P(VDF–TrFE)–LPSC	PVDF	1.2×10^{-3}, 25 °C	6 mA cm^{-2}, 200 h, 25 °C	3.7	[70]
PEGDME–LiTFSI	EO	$\sim1.5\times10^{-4}$, 60 °C	0.20 mA cm^{-2}, 2500 h, 60 °C	4.3	[31]
PEGDA–UpyMA–LiTFSI	EO	3.4×10^{-4}, 20 °C	0.20 mA cm^{-2}, 2500 h, 20 °C	5.2	[34]
PMMA–LLZTO–LiTFSI	MA	12.0×10^{-4}, 25 °C	0.10 mA cm^{-2}, 6000 h, 25 °C	–	[75]

electrolytes, Li^+ (from lithium salts) transport is related to the segmental motion of the ethylene oxide (EO) unit from the PEO chains, the motion can create free volume for the lithium-ion hopping from one coordinating site to another.[16] PEO has a high dielectric constant and strong Li^+ dissociation ability from lithium salt realizing continuous lithium ion hopping above the glass transition temperature (T_g). However, there are two main issues for PEO-based electrolytes: 1) the strong ionic bond –C–O– coordinated in the PEO chains between O atom and lithium ions restrict the ionic conductivity ($<10^{-7}$ S cm^{-1}) and lithium-ion transference number at room temperature; 2) higher glass transition temperature, resulting in high crystallinity at room temperature, which limits the movement of chain

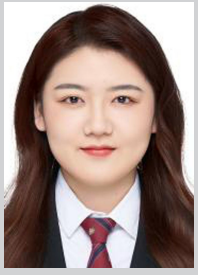

Xiaoxue Zhao is currently a Ph.D. student supervised by Prof. Fan at the University of Science and Technology Beijing. She received her M. S. degree in the School of Material Science & Engineering from China University of Geoscience Beijing. Her current research interests focus on organic and inorganic composite all-solid-state batteries.

Professor Li-Zhen Fan is the director of the Advanced Energy Materials Lab of the University of Science and Technology Beijing, China. She received her Ph.D. degree in Materials Science and Engineering from Tsinghua University in 2004. She worked as a post-doctoral research fellow at Kyushu University from 2004 to 2005, and then she worked as an Alexander von Humboldt fellow at the Max Planck Institute for Solid State Research from 2005 to 2007. She was a visiting scholar of Prof. John B. Goodenough's group at The University of Texas at Austin in 2014. Her research interest focuses on solid-state Lithium batteries, and she has co-authored more than 200 relevant peer-reviewed publications.

segments; 3) the limited electrochemical window stability below 4 V.

The PEO derivatives with block copolymers have raised special attention because they not only improve lithium salt dissociation and ionic conductivity, but also take advantage of microphase separation to balance the two antagonistic properties of ion transport and mechanical stiffness.[22,23] Nanostructured block copolymer electrolytes (BCE) have a promising applications in polymer electrolyte design, such as polystyrene-*block*-poly(ethylene oxide) (SEO) with the polystyrene block offering mechanical stiffness, and the PEO block solvates lithium salt and derived ions transport from lithium bis(trifluoromethansulfonyl)imide (LiTFSI).[24] Danie et al. prepared polystyrene-*block*-poly(ethylene oxide) (SEO–LiTFSI) and PEO–LiTFSI for experimental analysis to quantify the conductivity and ion dynamic transport mechanism in PEO-based bulk copolymer electrolyte.[25] By optimizing the ratio of EO : Li, the optimal concentration and ionic characteristics (such as ion solvation, correlation, and ion distribution) are revealed, as shown in Figure 2(a and b). Although the PEO–LiTFSI already reaches the maximum at the solvation site, the conductivity of SEO–LiTFSI remains constant, which means the proportion of the composite and uncomplicated EO units remains constant. The presence of non-conductive components in the periodic structure of block copolymer electrolyte (SEO–LiTFSI) can affect the solvation and transport characteristics of the entire bulk's conductive component.

Plasticizers as additives can serve as organic solid fillers to affect the crystallization behavior by increasing the proportion of amorphous phases and decreasing the glass transition temperature (T_g).[26] Succinonitrile (SN) as the one of typical plasticizers is reported widely.[27] Low molecular weight polymers and ionic liquids are also introduced to suppress the PEO crystalline phase. For example, Ran et al. crosslinked a hydrolyzed polymaleic anhydride (HPMA) low-molecular polymer plasticizer with PEO and lithium salt by a solution casting method in Figure 2(c).[28] Physical entanglement between HPMA and PEO, and –COOH group on the HPMA succeeded in weakening the crystallization and amorphous phase of PEO, improving the ionic conductivity. The ionic liquid usually promotes interfacial ion diffusion, but it may be a safety problem needed to further consider the liquid flammable plasticizer.

The physical mixture between polymer materials and inorganic filler is negligible for improving the PEO electrolytes because the Li^+ diffusion channel from polymer to the inorganic particle to polymer is discontinuous. Therefore, it is of great significance to embed additional lithium-ion pathways between inorganic fillers and polymers effectively achieving high ionic conductivity. The cyclodextrin is introduced in the

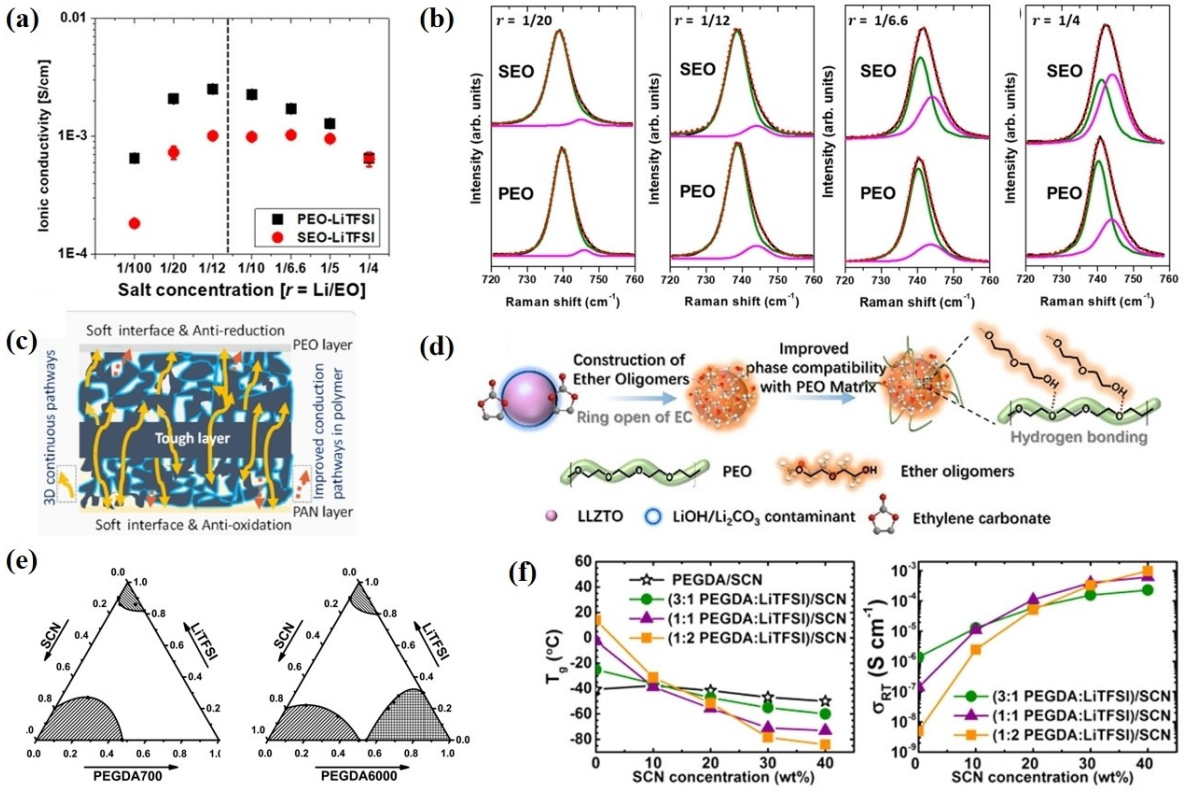

Figure 2. a) PEO–LiTFSI and SEO–LiTFSI as a function of salt concentration-conductivity at 100 °C ; b) Raman spectra for SEO–LiTFSI and PEO–LiTFSI films at salt concentrations [The dissociated "free" (green) and associated ion species (purple)]. Adapted with permission from Ref. [25]. Copyright (2021) American Chemical Society. c) Schematic diagram of sandwich structure solid electrolyte and SEM of its framework. Adapted with permission from Ref. [28]. Copyright (2021) Elsevier B.V. d) The interaction mechanism of LLZTO with EC in PEO. Adapted with permission from Ref. [30]. Copyright (2021) Wiley-VCH GmbH. e) Ternary phase diagram of PEGDA700 and PEGDA6000 blends at 25 °C. Adapted with permission from Ref. [37]. Copyright (2015) Elsevier B.V. f) DSC–Tg and room temperature ionic conductivity of various plasticized PEM systems. Adapted with permission from Ref. [38]. Copyright (2016) American Chemical Society.

polymer matrix and lithium salt, which not only are weaken the interaction between ether groups in PEO to fast Li^+ movement in the polymer matrix but also constructs a channel for Li^+ high-speed diffusion from PEO the matrix to LLZTO fillers to PEO matrix.[29] Similarly, He et al. creatively designed the intermolecular interaction between vinyl carbonate (EC) and active inorganic filler Ta doped $Li_7La_3Zr_2O_{12}$ (LLZTO) in P $(EO)_{15}$LiTFSI to solve the problem of poor room temperature conductivity of PEO based polymer electrolyte in Figure 2(d).[30] The ring opening reaction of EC initiated by LLZTO forms oligomers containing ether oxygen chains, which provides an additional rapid Li^+ conduction pathway. It also acts as a destructive agent of the PEO chain, which increases the amorphous phase region of Li^+ migration in PEO, and its room temperature conductivity reaches 1.43×10^{-3} S cm^{-1}.

The terminal hydroxide groups (–OH) are the limiting factor for PEO polymer oxidized in the voltage window 4.05–4.3 V. Esterification of unstable end group –OH of PEO generates poly(ethylene glycol)dimethyl ether(PEGDME), which is a cross-linked copolymer composed of conductive branched segments and a rigid matrix that can balance conductivity and mechanical properties, thus provides a satisfactory solid electrolyte membrane.[31] These polymers containing conductive branched chains are ideal components for the composite construction of solid electrolytes with other polymers. To solve the problem of cracks in polymer electrolytes during operation, Zhou and his colleagues innovatively formed a self-healing and highly tensile three-dimensional network through physical crosslinking of uracil (UPy) and PEGMA containing brush polyethylene glycol chain.[32] The cross-linked hydrogen bond network, electrolyte, and electrode contact show a stable effect of suppressing lithium dendrite (polarization current at 1 mAh, stable operation for more than 500 h), and making the abnormal high performance of solid-state battery (0.1 C, 80 cycles, capacity retention 91.6%). Similarly, Yao et al. also prepared PE film as a substrate-supported PEGMA composite solid electrolyte membrane with a thickness of 10 μm. The Li/PEGMA electrolyte/Li can stably operate over 1500 h at 0.1 mAh.[33] PEGDA is another polyethylene glycol (PEG) derivative with ether groups (–C–O–C–) on the chains, which has a shorter backbone and two C=C terminals bonds to introduce monomer for polymerization, it will cause a larger crosslink polymer network.[34] Generally, it acts as a curing agent to realize in-situ polymerization by UV photoinitiation. Wang and Dukjoon prepared poly(vinylidene fluoride) (PVDF) randomly dispersed with the PEGDA oligomer by solvent-controlled evaporation. PEGDA plays as curing to form an interpenetrating network with the PEO–PPO–PEO copolymers, facilitating mechanical strength, and assuring electrochemical up to 4.5 V.[35,36] To further improve the ionic conductivity and thermal stability, He and co-workers investigated the influence of the two kinds of PEGDA molecular weights and SN–LiTFSI concentration for photopolymerizing in the isotropic from the ternary phase diagram in Figure 2(e).[37] With the molecular weight of PEGDA increased from 700 to 6000 g mol^{-1}, the cross-linking point of the photopolymer reaction is decreased, which has higher ionic conductivity and flexibility. In addition, the glass transition temperature (T_g) rises as the concentration of lithium salt increases, which originates from the instantaneous physical cross-linking of ion–polyether oxygen coordination bonds and the chemical cross-linking of the PEGDA network (Figure 2f).[38] When its concentration get to 30 wt%, which reaches the threshold concentration of solution, the ether oxygen bond in the complex network is saturated, and T_g hardly increases.

Lithium salt in SSE, especially in polymer-based an important carrier source. The chemical composition and structure of lithium salt significantly influence the ion transport mechanism and interfacial stability of polymer-based SSEs. The most common lithium salts are perfluoroimide lithium salts containing fluorosulfonyl groups (e.g., LITFSI, LIFSI, LiFTFSI, etc). Zhang et al. systematically discussed the effects of three lithium salts on PEO-based electrolytes and confirmed that LITFSI has the highest ionic conductivity and low crystallinity.[39] LiFSI has stable cycling performance because of the stable LiF layer at the interface between LiFSI and Li metal after cycling. Furthermore, Meng et al. dissolved high-concentration LiTFSI in polyvinyl acetal (PVFM) boron-based single ionic conductor polymerization (LiPVFM), and designed a new "salt-with-salt" double lithium salt polymer solid electrolyte.[40] LiPVFM with a six-membered ether ring is beneficial to dissociate ions in lithium salt, and a rigid backbone can reduce T_g of electrolyte. In addition, lithium difluorooxalate borate (LiDFOB) has a wide electrochemical window and high conductivity and is often introduced into polymer-based SSE as an additive. The Cui group introduced LiDFOB into SPEs, it not only acted as a lithium source but also participated in the construction of an interfacial stable layer.[41]

2.2. Poly(acrylonitrile)-based polymer electrolytes

Poly (acrylonitrile) based polymer materials have a rich electron polar group and rigid bond called cyanide (–C≡N), which can improve mechanical strength and thermal stability.[42,43] The functional group nitrile of polyacrylonitrile (PAN) facilitates the construction and evolution of interfacial phases at the negative electrode/electrolyte, interface including solid electrolyte interphase (SEI) and cathode-electrolyte interface (CEI).[44,45] PAN is often used as the polymer substrate of rigid skeletons or extended electrochemical windows.

PAN can be weaved by the skeleton nanofiber as a solid electrolyte membrane with excellent mechanical strength and thermal, as well as flexibility. Generally, compared with traditional nanofibers, PAN fibers prepared by electrospinning have excellent mechanical properties and are preferred for further material composition.[46] Ye and his colleagues synthesized a kind of continuous nanoparticles of carbon and sulfurized PAN by single-hole electrospinning. The retention rate of 400 cycles in a lithium-sulfur battery was 60%.[47] Further mechanism analysis shows that the formation of an ionic conductive network of vulcanized PAN is the key to excellent electrochemical performance. It can not only avoid the side reaction between S and carbonate solvent but also adapt to the volume change of the cathode material. Such a successful example

inspired the design and manufacture of further similar polyacrylonitrile solid electrolytes. Zhang reported a sandwich membrane of PVDF–HFP and PAN as a solvent-free solid electrolyte supporting the skeleton.[48] The PAN nanofibers between the nanofiber membranes effectively controlled the growth of lithium dendrites, the lithium-ion batteries have good capacity retention of 82% after 400 cycles. Generally speaking, PAN is semicrystalline at room temperature, so the ionic conductivity of PAN electrolytes is very low.[49] The well-fabricated PAN polymer materials provided effective Li^+ conductive channels and a superior carrier incorporated with high-load ceramic electrolytes or the kinds of molecular structure polymer materials. PAN and metal-organic framework (MOF) particles are prepared as a composite solid electrolyte with thermal stability and good mechanical, and high ionic conductivity ($\sim 2.8\times10^{-4}$ S cm^{-1}) compared to pure PAN electrolyte.[50] PAN/MOF builds a 3D continuous interconnected ion conductive pathway and contributes to providing structural reinforcement (Figure 3a).[51] PAN is appropriately modified with other polymer materials on a molecular scale to improve ionic conductivity. Wang *et al.* reversed the traditional polyacrylonitrile-based composite electrolyte as follows.[65] Triacrylonitrile diacrylate crosslinked polyacrylonitrile polyethyleneimine (PAN–PEI) was used as a nanofiber membrane to prepare a solid electrolyte membrane by electrospinning (Figure 3b).[52] The nitrile from PAN undergoes amidation reactions compounded with PEI, as well as the PEI also provides an acidic site in the solvent. This unique crosslinking structure not only makes use of the branch PEI of the flexible skeleton but also helps to improve the mechanical properties of the fiber membrane. The tensile strength of the optimized PAN–PEI solid electrolyte membrane is 9.36 MPa and ionic conductivity at room temperature is 3.39×10^{-4} S cm^{-1}.

The $-C\equiv N$ group has a strong electronegativity, which can attract Li^+ in lithium salt and transition metal ions in cathode materials. PAN with viscosity and oxidation resistance is also an essential polymer as a coating layer material. Chen et al. reported a thin-film coating PAN on the particle surface of LLZTO by the solvothermal reaction process.[53] The uniform nanocoating of PAN-fabricated thin-film solid electrolytes improved the Li^+ transference number to 0.66, leading to a sufficient ionic conductivity of 1.1×10^{-4} S cm^{-1}. It is noted that

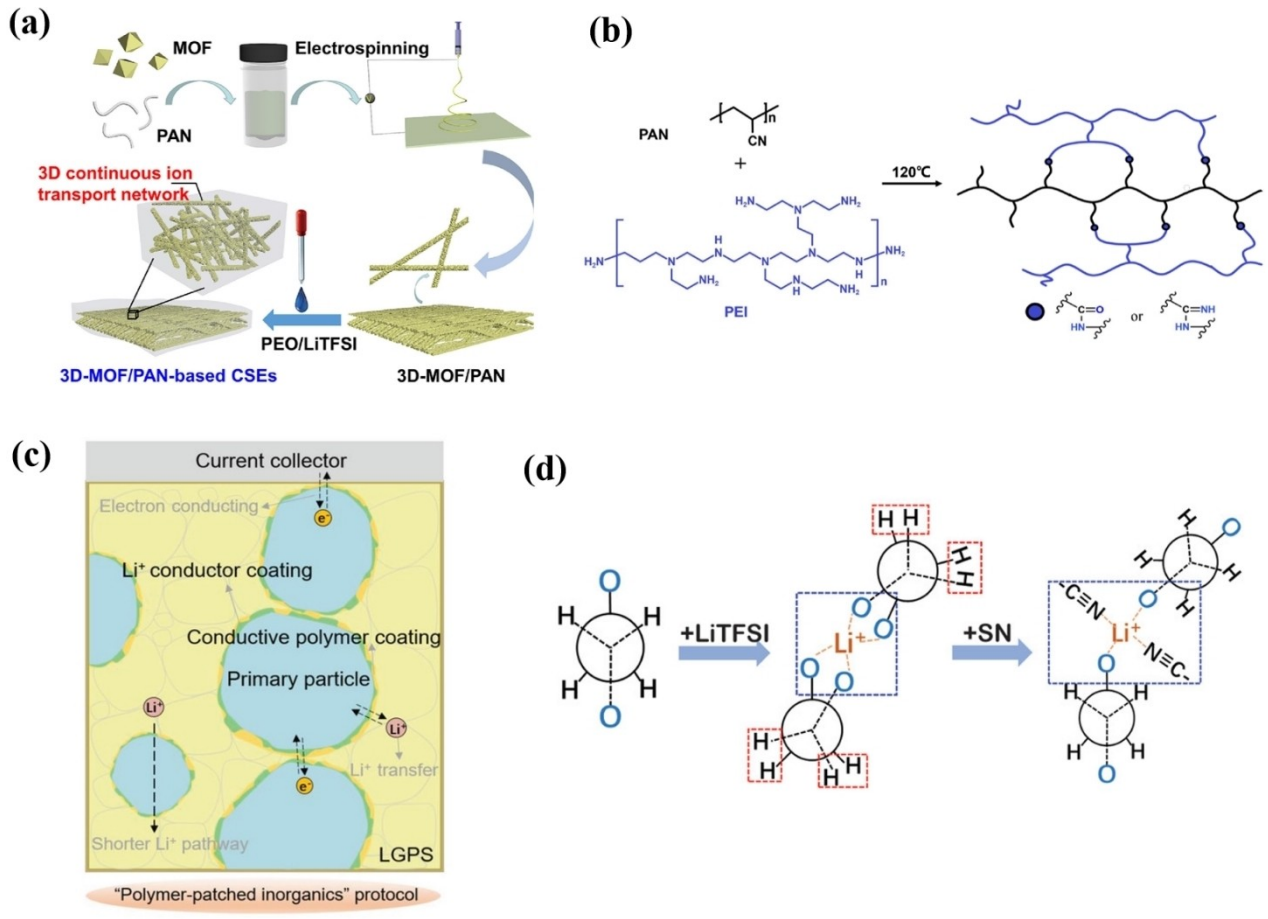

Figure 3. a) Schematic procedure to fabricate 3D interconnected MOFs-based CSEs. The 3D interconnected MOF/PAN network was prepared by electrospinning the mixture solution of MOFs and PAN. Adapted with permission from Ref. [51]. Copyright (2022) Elsevier B.V. b) The schematic diagram of the crosslinking reaction between PAN and PEI. Adapted with permission from Ref. [52]. Copyright (2021) Elsevier Ltd. c) Schematic illustration of "polymer-patched inorganic" coating protocol surpassing the typical interface engineering. Adapted with permission from Ref. [57]. Copyright (2022) Wiley-VCH GmbH. d) Carbon conformation transition diagram of PEO, and SN–PEO of SPEs. Adapted with permission from Ref. [60]. Copyright (2020) Wiley-VCH GmbH.

when PAN is heated at 300 °C, a cyclization reaction will occur to generate cyclized PAN (c–PAN), whose delocalized π bonds are promoted to construct a connection with cathode particles.[54,55] Wang et al. constructed a coating layer with high conductivity, dense regularity, and ion permeability.[56] The PAN is coated on the surface of the NCM811 particles, and a bridge layer is rock salt, which transforms from the surface layer phase with charging/discharging cycles. It provides a new protocol to solve the electrochemical-mechanical degradation of NCM cathode particles in long cycles. Liang et al. introduced cyclized PAN (c–PAN) and nanoscale $Li_{1.4}Al_{0.4}Ti_{1.6}(PO_4)_3$ (LATP) coated on the single-crystalline $LiNi_{0.6}Co_{0.2}Mn_{0.2}O_2$ (SNCM) cathode particles in Figure 3(c).[57] Homogeneous coating layer, especially PAN with delocalized π bond, extended electronic contact with SNCM particles, delivering a good electrochemical performance of capacity retention (72.7% over 500 cycles, at 0.5 C). Meanwhile, Jiang et al. used theoretical models and simulation to reveal that PAN as a coating layer is beneficial to accelerate the diffusion of Li+ to cathode particles. It also has a stress-buffering effect coupled with the PVDF binder.[58]

Succinontrile (SN) also contains cyano groups as an effective additive for solid-state batteries.[59] The –C≡N groups can interact with a lithium salt and another polymer. The PEO-SN systems can form a fast Li^+ transport pathway without lithium salt. Xu et al. analyzed the NMR spectra that adding a high content of SN(SN:EO = 1:4) can construct fast ion channels for homogeneous solid-state electrolytes in Figure 3(d).[60] In addition, PAN and SN can form a stable interface with lithium metal, which will be discussed in Section 5.

2.3. Poly(vinylidene fluoride)-based polymer electrolytes

Poly(vinylidene fluoride) (PVDF) and its copolymers are also semi-crystalline structure polymers, which are classified by α, β, and γ-phase. In these polymorphs, α and β-phase of PVDF are commonly used by the solid-state electrolyte. α-phase is thermos-dynamic stable and non-polar, β-phase applied for piezoelectric, pyroelectric, and ferroelectric with a high dipolar moment of 7×10^{-30} cm.[51] PVDF and its copolymers as solid electrolytes process high mechanical strength, a wide electrochemical window, and thermal stability.[18] This chapter will focus on PVDF, PVDF–HFP, and PVDF–TrFE for solid electrolytes according to recent progress.

PVDF polymer is a promising solid electrolyte material due to superior chemical stability and dielectric constant. In the PVDF-based electrolyte, the residual solvent of N, N-dimethylformamide (DMF) could play a critical role in the lithium transport, interface stability, and the performance of batteries. Nan's group investigated the effect of the resident solvent DMF concentration on the chemical reaction mechanism and ionic conductivity (Figure 4a).[62] The amount of resident solvent DMF is controlled at the range from 10–14 wt% in the PVDF-based solid electrolyte, where interaction sites between $[Li(DMF)_x]^+$ and PVDF chains transport (Figure 4b). In the PVDF–DMF solution, the DMF is complexed with Li ions with no free solvent. By varying the fillers, and polymer function group composition of PVDF-based electrolytes, the lithium-ion conductivity can be improved. Chen et al. introduced Y^{3+}-doped $Li_{29}Zr_9Nb_3O_{40}$ (LZNO) active fillers into the PVDF electrolyte.[63]

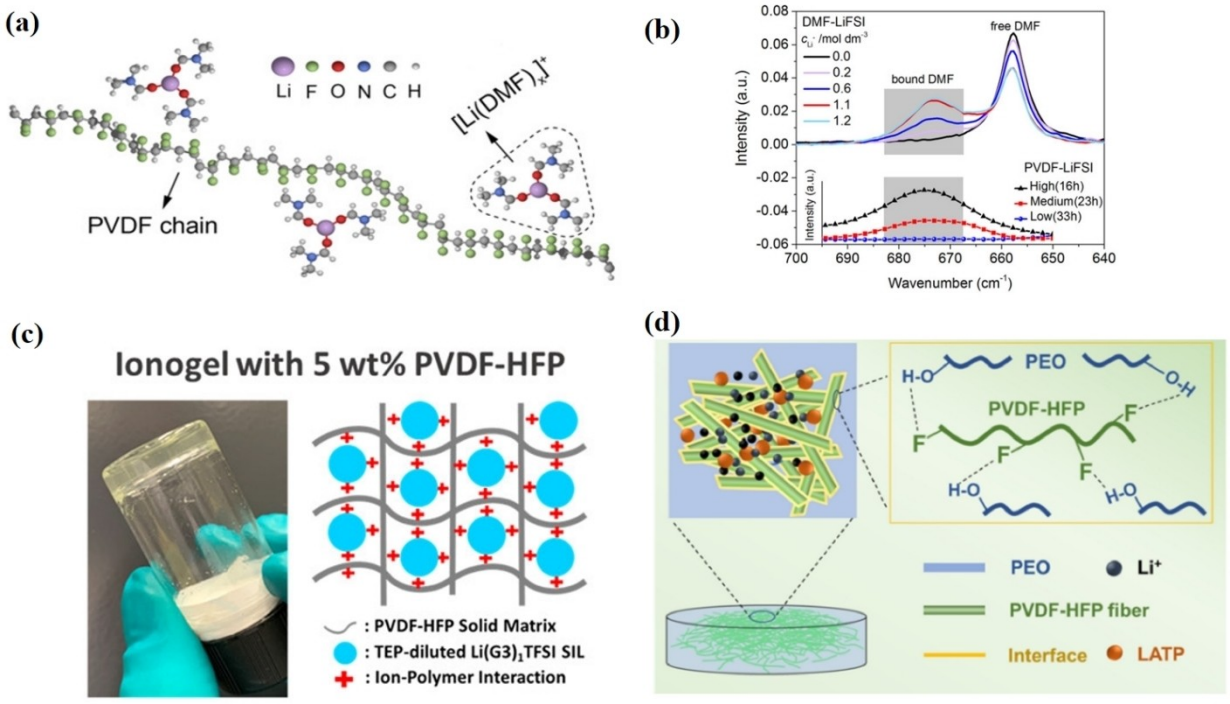

Figure 4. a) $[Li(DMF)_x]^+$ ($x \leq 3.29$) in the PVDF–LiFSI electrolyte; b) FTIR spectra observed for DMF–LiFSI solutions with various salt concentrations and different vacuum drying times. Adapted with permission from Ref. [62]. Copyright (2020) Wiley-VCH. c) The interaction between ion gel with 5 wt % PVDF–HFP. Adapted with permission from Ref. [66]. Copyright (2022) American Chemical Society. d) Intermolecular hydrogen binding effect between PVDF–HFP and PEO. Adapted with permission from Ref. [67]. Copyright (2021) Elsevier Ltd.

The high dielectric constants of PVDF and Y^{3+} benefit to promote the lithium salt dissociation, the ionic conductivity from 1.26×10^{-4} S cm^{-1} to 2.34×10^{-4} S cm^{-1} at room temperature was achieved. Tsai et al. investigated the poly (styrene sulfonic acid) (PSSA) chains grafted on the surface of PVDF porous electrolyte membranes.[64] With ion conductor-containing chains, the PVDF porous electrolyte membranes have a higher ionic conductivity, because the situ-polymer at the surface constructed Li^+ conductivity pathways and electrochemical stability than the neat PVDF support.

PVDF–HFP can also dissociate a large amount of lithium salt to obtain high ionic conductivity, it has excellent flexibility and dielectric constant up to 8.4, which related to a semi-crystalline polymer structure and additional hexafluoropropylene (HFP), compared to PVDF.[65] Li et al. combined the PVDF–HFP (as a solid matrix) with LLZO, LiTFSI, triglyme, and triethyl phosphate to develop bipolar SSBs (Figure 4c).[66] The interaction of PVDF–HFP and ion gel constructed the ion/plasticizer-polymer, with a remarkable ionic conductivity at room temperature 2.61×10^{-3} S cm^{-1}. In addition, the bipolar SSB can stable operate even at −18 °C and tolerant cutting, burning, and folding. Besides, the PVDF–HFP nanofiber has also been introduced as a host supporting created a 3D framework. Yao et al. prepared a thin and high-performance composite solid electrolytes membrane by electrospinning and a subsequent hot-press process with PEO and LATP particles (Figure 4d).[67] The PVDF–HFP nanofibers can interact with PEO formed the H–F bond at the 60 °C molting, it had 50 μm thickness and provided a high electrochemical window of 5.2 V, the lithium transference number is 0.49 at 60 °C, and can stable cycle with 94.6% capacity retention at 0.1 C after 100 cycles.

Poly(vinylidene fluoride–cotrifluoroethylene) [P(VDF–TrFE)] has a polar ferroelectric transplanter chain conformation and all urine atoms are located on one side, hydrogen atoms are positioned on the other side of the chain. The crystalline structure is similar to the b-phase of PVDF.[68] P(VDF–TrFE) is a unique ferroelectric polymer that can promote lithium salt dissociation to form more free charge carriers and lithium ions mobility. He's group introduced copolymer poly(vinylidene fluoride-co-chlorotrifluoroethylene) [P(VDF–TrFE–CTFE)] as the polymer matrix to form novel SPEs.[69] The ferroelectric polymer structure copolymer electrolyte created a high ionic conductivity of 3.1×10^{-4} S cm^{-1} at room temperature and a low activation energy of 0.26 eV compared with PVDF electrolyte (1.77×10^{-5} S cm^{-1} and 0.49 eV). In addition, P(VDF–TrFE) exhibits more flexibility than commonly used PVDF, which is suitable as a self-support skeleton combined with sulfide electrolytes to create ultra-thin and high-conductivity solid electrolyte membrane. Nan and his colleague constructed a three-dimensional poly(vinylidene fluoride–cotrifluoroethylene) P(VDF–TrFE) network composed of argyrodite Li_6PS_5Cl (LPSCl) by electrospinning-infiltration-hot-pressing method.[70] Interaction of polar P(VDF–TrFE) and LPSCl not only generates high ionic conductivities, but also produce good mechanical and reach the thickness of 30–40 μm.

2.4. Poly(maleic anhydride)-based polymer electrolytes

Maleic anhydride (MA) is an alternative polymer electrolytes with anhydride group and double carbon bonds. MA promotes the synthesis of poly(maleic anhydride)-copolymer, through the free radical polymer. Then, it can act as graft sites for amidation and esterification reactions to design anhydride polymers with different side chains.[19,71] Especially, polymethyl methacrylate (PMMA) regulation is a suitable polymer-based solid electrolyte for the adverse reaction of the lithium-mental electrode and with a higher lithium ion migration number.[72,73] For PMMA regulation, Zhou et al. integrated PMMA and polyvinylidene fluoride PVDF into an artificial SEI as a solid electrolyte membrane.[74] The introduced PMMA and polyvinylidene fluoride contribute to the formation of the lithium fluoride layer in situ and lithium-ion bond in situ, and provide a channel for lithium-ion transmission, further adjust the lithium-ion distribution and restrain the growth of dendrites. The modified solid electrolyte can operate stably for 500 h when the polarization current is 1 mAh cm^{-2}. PMMA also acts as a nanopore template combined with LLZTO to synthesize 3D frame structure by assisted sintering to obtain excellent lithium ion transmission performance.[75] An in-depth analysis shows that a continuous conductive network can provide high ionic conductivity. Moreover, the filling of the solid electrolyte and the combination of a dense polymer layer on the outer surface can block the path of lithium dendrite and obtain excellent electrochemical performance (when the polarization current potential is 0.1 mAh cm^{-2}, it can cycle stably for more than 1600 h).

In summary, ether oxygen groups (EO) and soft macromolecular chains are favorable to promoting lithium salt dissociation, and high conductivity above T_g temperature. But the terminal group is thought limited to the electrochemical window, and could use some modification. Cyanide (–C≡N) groups with a rigid bond act as a backbone to increase the self-supporting properties of the SPEs membrane and have a wide electrochemical window. The ionic conductivity is not as good as that of PEO-based polymers. PVDF and its copolymers have good mechanical properties, and its ferroelectric properties facilitate lithium salt dissociation. Maleic anhydride (MA) has –C=C and anhydride groups, with suitable anchor points for grafting with other polymers or functional side chains to meet applicational requirements.

3. Chemical and Electrochemical Dynamic Mechanism of Polymer-based Solid-State Electrolytes

Generally speaking, there are two conduction mechanisms of lithium ions in the solid electrolyte: one is the movement of ions in vacancies and gaps, and another is the fracture and formation of an amorphous coordination bond in the movement of local segments of the polymer.[77] Specifically, ionic conductivity is related to carrier concentration, ionic mobility, and ionic charge.[78] In solid electrolytes, the general description

formula of ionic conductivity is as follows:

$$\sigma = \sum u_i \cdot q_i \cdot c_i$$

Where u_i is the ion mobility, q_i is the ion charge and ci is the carrier concentration. In the solid electrolyte system, the ion mobility u_i is related to the glass phase transformation of the polymer in the amorphous phase. When a solid electrolyte has a lower glass transition temperature (T_g) and a more amorphous state, it is conducive to the conduction process of lithium ions. In addition, the carrier concentration c_i is complex in improving the conductivity, which is mainly discussed in three parts: 1) The concentration of lithium ions dissolved in the polymer; 2) ion-dipole interaction between salt and polymer (Lewis acid-base); 3) the plasticizing effect of salt on the polymer host reduces the crystallinity of the polymer body (plasticizer, vacancy).[79] Therefore, glass transition temperature, lithium salt concentration, and other parameters affect the complex interaction between lithium ion and polymer functional groups, and the ionic conductivity of solid electrolytes.

The electrochemical stability window of solid electrolytes refers to the voltage range that can be maintained without redox decomposition in the process of charge and discharge. For the cathode-electrolyte interface side, the HOMO maximum orbital potential of polymer/inorganic filler, lithium salt, and additive in the solid electrolyte is required to be lower than the cathode material. The high voltage stability of a solid electrolyte is determined by its anion framework, and ability to lose electrons, which are limited by the anion ionization potential.[80] However, the high-voltage lithium metal battery is more complex in charge and discharge. A portion of the cathode material contains transition metal ions whose highest molecular orbital potential μ_c may jump to a lower orbital, during redox, leading to interfacial parasitic reactions.[8] The stability of the lithium metal anode is determined by the ability of the solid electrolyte to accept electrons. The lithium metal electrode-electrolyte interface is mainly divided into two parts: The problems of the lithium metal interface during charge-discharge include 1) uneven ions deposition due to chemical parasitic reactions; 2) the growth of dendrites, punctures, and crack extensions.[81,82] When the local distribution of impurity particles form solid electrolytes is not uniform at the lithium-metal interface, the rugged components would consume lithium metal. And then interface parasitic reaction continues reacted solid electrolyte components resulting in insufficient electrode-electrolyte interface contact.[9] In addition, the crack propagation of lithium dendrite at the grain is also concerned at the lithium/electrolyte interface. In general, lithium dendrite growth and dendrite piercing should be taken into account for solid-state electrolyte coupling effects.

4. Strategies of Polymer-based Composite Solid-State-Electrolyte

In polymer-based solid electrolytes, ion transport and mechanical performance are concerned usually. In recent research, there are three ways to increase the ion transport pathway for improving ionic conductivity (Table 2): 1) the polymer chain can be modified by incorporating passive fillers; 2) active fillers incorporated with the polymer can construct lithium-ion transport pathway; 3) metal/Covalent organic frameworks can build continuous phase pathways or three-dimensional skeletons. Therefore, ceramic incorporated with polymer solid electrolytes has attracted interest to enhance ionic conductivity.

4.1. Inert filler

The crystallinity of the polymer is one of the important factors affecting ionic conductivity. The addition of inert fillers is a feasible way to improve ionic conductivity, which facilitates the reduction of the crystallinity of the polymer matrix and promotes the dissociation of lithium salts.[92,93] Inert fillers, involving SiO_2, TiO_2, Al_2O_3, etc, can increase the free volume of the polymer matrix and accelerate the dynamics of the polymer block resulting to decrease polymer crystallinity and T_g of polymer. Lin and his colleagues carried out pioneering work and proposed a method to synthesize composite solid electrolytes by using SiO_2-aerogel as the framework for polymer-based electrolytes (Figure 5a).[84] SiO_2 ultrafine particles are uniformly distributed in the polymer matrix electrolyte, which has a relatively large specific surface that can provide more active sites with the functional groups of organic molecules, and form a continuous aerogel network conducive to enhanced mechanical properties. The interaction between fillers and polymers also enhanced the dissociation of lithium salts and improves the ionic conductivity of the overall composite solid

Table 2. Summary of performance of organic-inorganic composite solid-state electrolytes.

Filler	Polymer/Salt	Conductivity [S cm^{-1}]	Voltage Window [V]	Ref.
SiO_2	PEO/TDI	1.2×10^{-4} (25 °C)	5.6	[83]
SiO_2 aerogel	PEGMA/PEO/LiTFSI	6.0×10^{-4} (30 °C)	–	[84]
TiO_2-grafted NHPE	PEGMEM/LiTFSI	1.1×10^{-4} (30 °C)	5.4	[85]
Al_2O_3 fillers	PVDF–HFP/PEG/LiTFSI	8.3×10^{-4} (30 °C)	–	[86]
LLZO	PEO/LiTFSI	1.1×10^{-4} (30 °C)	5	[87]
LLTO	PVDF–HFP/LiTFSI	1.2×10^{-4} (30 °C)	4.7	[88]
LLTO–LLZO	PVDF–PTFE	1.4×10^{-4} (30 °C)	5.3	[89]
3D-PAN/LLZTO	PEO/LiTFSI	2.3×10^{-4} (30 °C)	5.2	[90]
LATP/PE	PEO/LiTFSI	1.4×10^{-4} (60 °C)	–	[91]
MOF	PAN/PEO/LiTFSI	2.9×10^{-4} (25 °C)	4.7	[51]

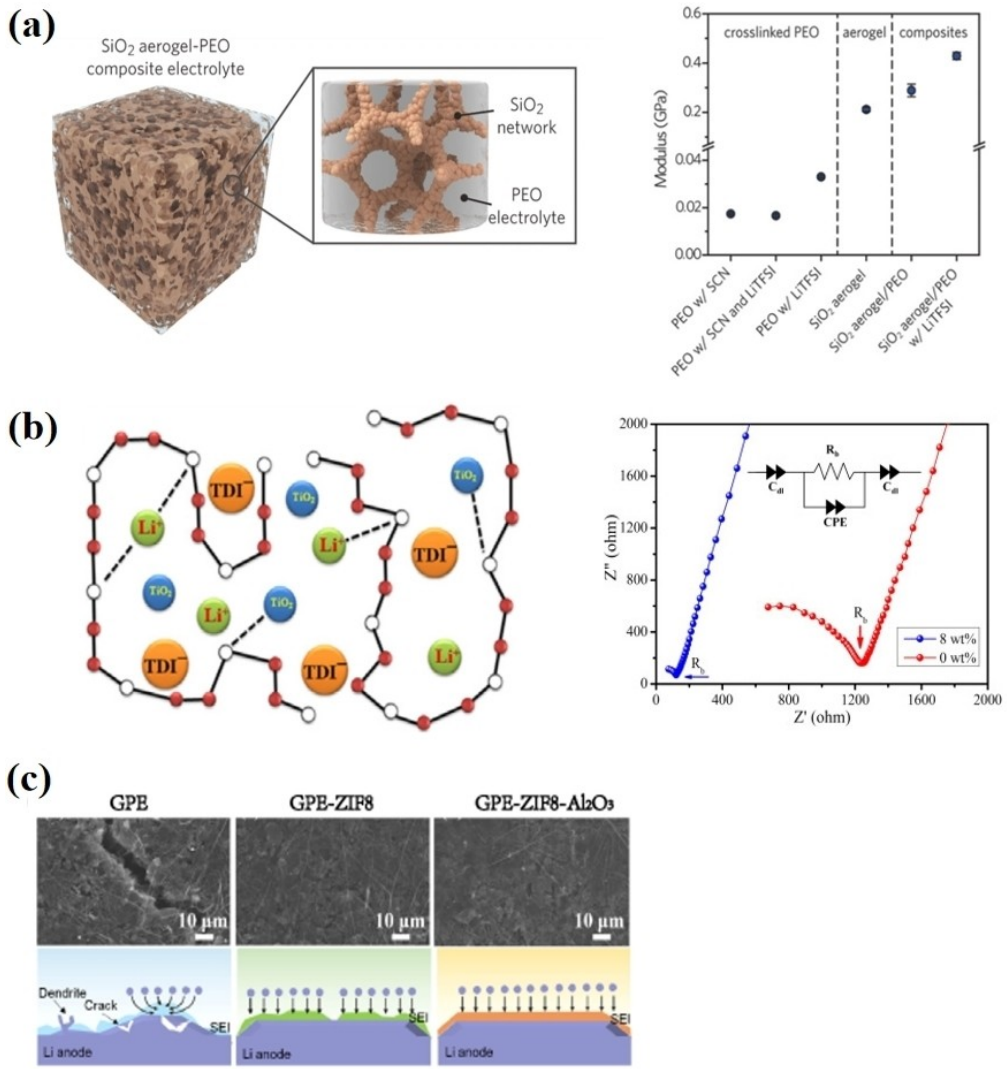

Figure 5. a) SiO_2-aerogel as a skeleton-reinforced composite solid electrolyte and elastic modulus. Adapted with permission from Ref. [84]. Copyright (2018) WILEY-VCH. b) Nyquist impedance plots of PEO12–LiTDI and PEO 12-LiTDI-8 wt% TiO_2 electrolyte membranes at room temperature. Adapted with permission from Ref. [96]. Copyright (2016) The Korean Society of Industrial and Engineering Chemistry. Published by Elsevier B.V. c) Surface morphologies of lithium deposition, and schematic diagrams after cycling with GPE/Al_2O_3. Adapted with permission from Ref. [97]. Copyright (2022) American Chemical Society.

electrolyte(6×10^{-4} S cm^{-1}, 30 °C). For the practical application of SiO_2 filler composite with polymer-based SSEs. Li et al. further used the one-pot synthesis strategy to effectively crosslink SiO_2–PEO through the bridging action of toluene diisocyanate (TDI) forming a polymer-inorganic crosslink.[83] Due to the active groups –NCO on the TDI surface, the obtained electrolyte membrane has a strong connection between PEO chains and SiO_2 showing superior electrochemical performance at room temperature (1.2×10^{-4} S cm^{-1}).

TiO_2 is also chosen as a polymer electrolyte filler on account of its special shape and surface properties.[94,95] Recently, Chen and colleagues effectively increased the interface contact by introducing TiO_2 nanofibers into the lithium metal-LLZTO electrolyte interface (Figure 5b).[96] Compared with the unregulated interface, TiO_2 significantly reduces the interface resistance (from 374 Ω cm^{-2} to 27 Ω cm^{-2}) and improves the cycle performance of solid-state batteries. In addition, TiO_2 effectively interferes with the orderly stacking trend of the host polymer chain and reduces its crystallinity.

Al_2O_3 is a commonly inorganic filler to graft polymer through Lewis acid-base promoting the dissociation of lithium salt and increasing the wettability of the lithium metal interface (Figure 5c).[97] Recently, Al_2O_3 was proposed to be dispersed in polymer electrolytes as an inorganic filler.[98] Specifically, the addition of Al_2O_3 filler showed expected ionic conductivity (5.26×10^{-3} S cm^{-1}). TiO_2 particles are encapsulated by PVDF–HFP, similar to plasticizers being trapped in a polymer electrolyte matrix, which provides a good transport pathway for lithium ion transport for the polymer material.

Although progress has been achieved for inert filler-polymer composite SSEs, some issues have not yet been solved: 1) the inert filler doesn't change the conductivity mechanism of the polymer electrolyte, it is limited to improve the ionic conductivity; 2) nanoparticles are easy to agglomerate or

disperse poorly exposed little active sites, which makes it difficult to combine with polar groups and anions; 3) in the inert-filler particles, segmentation dynamics and ionic conduction are blocked resulting in lower ion transport and ion transfer numbers.

4.2. Active ceramic filler

Compared to inert fillers, active fillers are incorporated with polymers to generate organic-inorganic composite SSEs, therefore provides more lithium ion conduction pathways.[99] In active filler, the ions transport mechanism mainly depends on Li^+ migrating in the crystalline phase and jumping between them, resulting in a percolation path. In particular, the migration energy (E_a) is mainly influenced by the grain boundary morphology of ceramics. When polymers are the main phase, the ionic conductivity will change with the environment temperature. Active fillers are the main conductive medium, and polymers act as a binder for cross-linking and adhesion. It forms three different ion transport paths in the composite electrolytes.[100,101] Specifically, there are three-phase conduction mechanisms in the inorganic-organic composite SSE, including active filler conduction, polymer/filler interface conduction, and polymer (lithium salt) conduction.[102] Therefore, more work focused on improving the ionic conductivity of polymer-based SSEs by incorporating active fillers. Generally, active fillers are researched including the garnet structure oxide of $Li_7La_3Zr_2O_{12}$ (LLZO) and $Li_{6.4}La_3Zr_{1.4}Ta_{0.6}O_{12}$ (LLZTO),[103] the perovskite structure oxide of $Li_{3x}La_{2/3-x}TiO_3$ (LLTO),[104] and the fast ionic conductor of sodium superionic conductor(NASION).[105]

4.2.1. Garnet structure oxide–LLZO

Garnet structure electrolytes with Li7 phase are a general formula of $Li_7La_3Zr_2O_{12}$(LLZO), lithium-ion is distributed in the interstitial sites of the tetrahedral (24d), octahedral (48 g), and octahedral (96 h). The garnet crystalline structure can accommodate the excess of lithium cations, which leads to ionic conductivity of 10^{-4} S cm^{-1} at room temperature.[106] $Li_7La_3Zr_2O_{12}$ can form new conductive pathways in the crystal structure, however, its agglomeration often fails to have enough active sites to cross-link with the anion, which affects the room-temperature ionic conductivity. To form a continuous conductive network, Pan et al. performed the $Li_7La_3Zr_2O_{12}$ fiber with PEO and LiTFSI salt through a silk-template process (Figure 6a).[107] The accomplished composite electrolyte presents 2.4×10^{-5} S cm^{-1} ionic conductivity at room temperature. In addition to optimizing the ion conduction path, it is also necessary to closely consider adjusting the air-stable of $Li_7La_3Zr_2O_{12}$ to minimize the phase transition in the air and maximize its interface stability.[108] $Li_7La_3Zr_2O_{12}$ is sensitive to water and oxygen. Martin Finsterbusch et al. reported a recent work that systematically clarified the hydration mechanism of $Li_7La_3Zr_2O_{12}$ in a humid air.[109] Specifically, the amount of $Li_7La_3Zr_2O_{12}$ absorption increases with the increase of temperature before 200 °C, and the water absorption begins to stop after exceeding 200 °C. Li·H_2O generated at room temperature limits the surface diffusion of $Li_7La_3Zr_2O_{12}$, which affects the interface reaction of solid-state batteries. Ta-doped LLZO is an idea to stable the LLZO particles' surface.[110] Huo et al. constructed three different interfaces between LLZTO and Li metals, including the original interface, lipophilic interface, and three-dimensional structure interface. A new acid etching process was used to prepare LLZTO with a three-dimensional

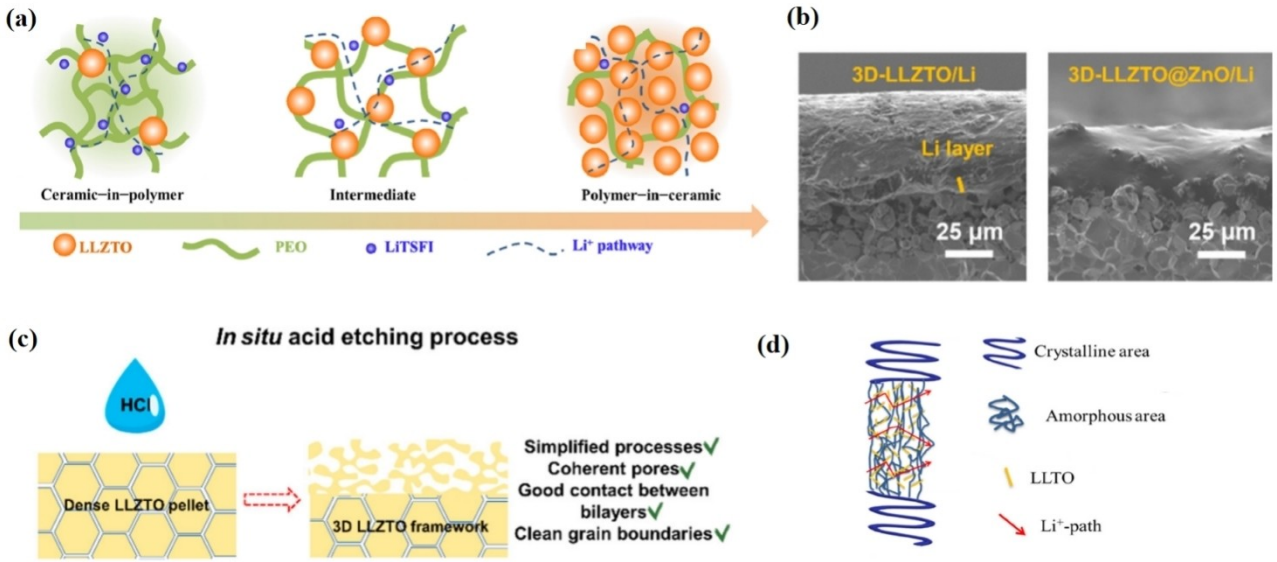

Figure 6. a) LLZO active filler conductive network. Adapted with permission from Ref. [107]. Copyright (2018) Elsevier. b, c) Schematic of the in situ acid-etching process, cross-sectional and top-view SEM images of 3D-LLZTO. Adapted with permission from Ref. [111]. Copyright (2020) American Chemical Society. d) Demonstration of the mechanism of Li^+ transmission path in the LLTO composite electrolytes. Adapted with permission from Ref. [88]. Copyright (2021) Elsevier B.V.

frame (Figure 6b, c).[111] Acid etching not only forms a situ uniform pore structure, but also removes the grain boundaries surface pollutants and impurities. From the perspective of production, the 3D skeleton thickness is controlled by the concentration of hydrochloric acid solution and etching time, which is conducive to large-scale production. The room temperature conductivity of the 3D-LLZTO composite SSE membrane is 8.2×10^{-4} S cm^{-1}. In terms of interfacial ion transport, Chen also constructed a gradient composite polymer electrolyte on the polymer substrate by simple UV curing technology.[112] The large elastic modulus of LLZTO layer can withstand the volume expansion of the PEO layer, ensuring that the electrolyte film is not bent or deformed.

4.2.2. Perovskite structure oxide–LLTO

Perovskites have the general formula of ABO_3 with cubic phase, where Li^+ partial substitution La^{3+} in $LaTiO_3$. $Li_{3x}La_{2/3-x}TiO_3$ (LLTO) is an attractive perovskite structure for SSE. Its conduction mechanism depends on its A-site vacancy, and the value of x plays a large role in its ionic conductivity.[113] Yan developed an asymmetric composite SSE membrane with high mechanical strain.[89] LLTO is covered at the interface to solve uneven current distribution at the Li metal interface. The room temperature ionic conductivity of the composite SSE membrane is 1.38×10^{-4} S cm^{-1}, and the Li–Li battery can stable cycle over 2000 h under the polarization current of 0.2 mA cm^{-2}. Similarly, Li et al. introduced LLTO nanorods into the PVDF–HFP polymer matrix as a new composite solid electrolyte. LLTO nanorods can provide a three-dimensional lithium ion transport path and increase free volume (Figure 6d).[88] Besides, the high mechanical properties and thermal stability of PVDF–HFP polymer make the composite solid electrolyte have high ionic conductivity (1.21×10^{-4} S cm^{-1}) at room temperature.

4.2.3. Fast ionic conductor-NASION

In addition to garnet and perovskite structures, fast ionic conductors (NASION) can also be introduced into polymers as active fillers to reduce their crystallinity, build conductive networks, and enhance conductivity and lithium-ion transfer number, such as $Li_{1.5}Al_{0.5}Ge_{1.5}(PO_4)_3$ (LAGP) and $Li_{1.3}Al_{0.3}Ti_{1.7}(PO_4)_3$ (LATP). LATP is proven to be a solid electrolyte material with higher performance because of its excellent mechanical properties and high Li^+ transfer number. Liu et al. manufactured a LATP–xBG dense ceramic electrolyte synthesized by LAGP and amorphous borosilicate glass (BG), which showed acceptable conductivity and mechanical properties (conductivity 10^{-4} S cm^{-1}).[114] To form a continuous 3D network of inorganic fillers in polymers, our group proposed a sacrificial template method, which introduced cheap and ordinary sodium chloride powder into polymers as sacrificial templates. Polyethylene oxide (PEO) and lithium salt (LiTFSI) were selected as fillers and introduced into 3D conductive networks.[115] Firstly, sodium chloride (NaCl) and fast ion conductor LATP powder were mixed, PTFE was introduced as an adhesive, and then the NaCl template was removed in water. The NaCl template is easily soluble in water and can be removed with water, the porosity of the three-dimensional conductive frame is easy to control. Additionally, the three-dimensional LATP framework can provide a continuous Li^+ conductive pathway and sufficient mechanical modulus, and promote the rapid transmission of Li^+ and suppress the growth of lithium dendrites. Therefore, the well-designed LATP–PEO SSE shows that it can operate stably for more than 1000 h at a polarization current of 0.2 mA cm^{-2}.

In conclusion, the combination of inorganic filler and polymer matrix can provide opportunities for the application of high-specific energy ASSBs through complementary regulation. In addition, LAGP has characteristics to the conductivity of liquid electrolytes at room temperature and good electrochemical stability, which has attracted much attention. Researchers proposed a series of LAGP composite SSE materials, including LAGP–PP membrane,[116] LAGP–PEO composite electrolyte, and LAGP–Li_3InCl_6 composite electrolyte.[117] In these works, it is also observed that there are side reactions and modification strategies at the interface between fast ion conductors and lithium metal, which will be focused on in the later section of lithium dendrite.

4.3. 3D organic/covalent network framework

Metal-organic framework and covalent organic framework materials provide a new direction for high-performance solid electrolytes. Theoretically, these materials have regular channels and a large specific surface area, which can provide pathways for the rapid conduction of lithium ions in SSEs.[118] In addition, the organic framework is the same as the polymer composite but with good flexibility, which can be practically processed and applied by a roll-to-roll process.[119]

4.3.1. Metal-organic frameworks

In metal-organic frameworks, there are three strategies to improve the ion conductivity of solid electrolytes: 1) as fillers incorporating with polymers solid electrolytes; 2) by confining ionic liquids within the MOF conductive frame; 3) construct unsaturated metal sites and dissociate lithium salts.[120] Li et al. found that the composite of MOF, PAN, and PEO showed excellent ionic conductivity and mechanical properties (Figure 7a).[51] From the perspective of microstructure and COMSOL simulation, the design of 3D-MOF/PAN enhanced the mechanical strength and uniform deposition of lithium effectively suppressed the growth of lithium dendrites, and also provided a continuous pathway for rapid Li^+ transport, improving the ionic conductivity and Li^+ transfer number. Great efforts have been made to introduce ionic liquids into metal-organic frameworks, especially to improve ionic conduction through the interaction between ions and MOFs or adjust the pore size

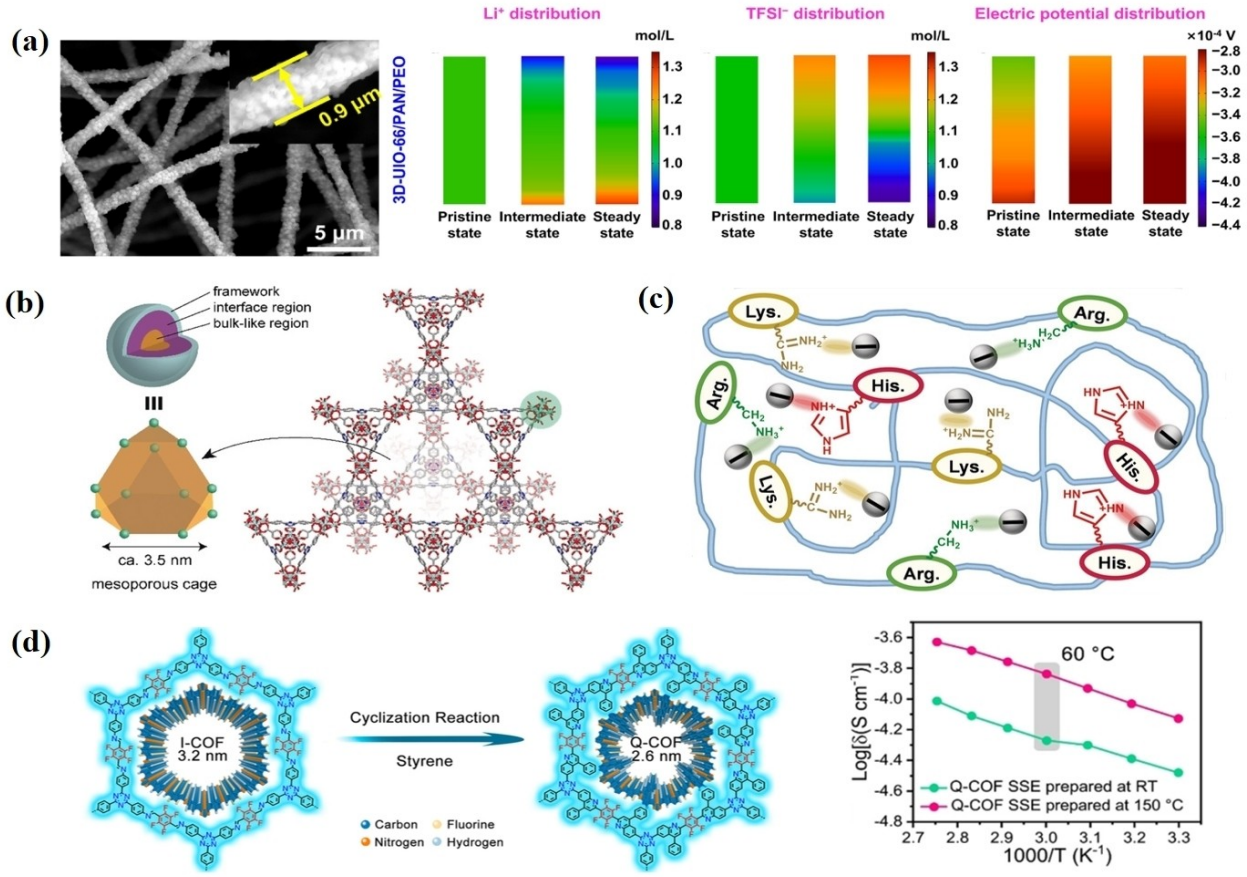

Figure 7. a) Rational design of 3D interconnected SSE based on MOFs. Adapted with permission from Ref. [51]. Copyright (2022) Elsevier B.V. b) IL–MOF (Zr)–3D skeleton network. Adapted with permission from Ref. [121]. Copyright (2019) Wiley-VCH Verlag GmbH & Co. KGaA, Weinheim. c) The transition of ions in protein chains. Adapted from Ref. [122]. Copyright (2022) The Authors. Advanced Science published by Wiley-VCH GmbH. d) Quinoline crosslinked COFs were synthesized by cyclization of highly crystalline imines combined with COFs. Adapted with permission from Ref. [123]. Copyright (2021) Wiley-VCH GmbH.

of MOFs. Yoshida et al. obtained a mesoporous cage with truncated tetrahedron by ligand connection of zirconium-based mesoporous MOF, which limits the ionic liquid composed of 1-ethyl-3-methylimidazole (EMI^+) cation and dicyandiamide ($n(CN)_2$@) anion (Figure 7b).[121] Further filling of the ionic liquid builds a large number of regions in pores of the MOF to achieve super-ionic conduction, thus the SSE provides a satisfactory room temperature conductivity of 4.4×10^{-3} S cm^{-1}. Directly constructing MOF conductive network and grafting with lithium salt is also a strategy. Gu et al. explored a recyclable and self-healing soybean protein isolate as the MOF dynamic skeleton. The introduction of lithium bis(trifluoromethane)sulfonimide (LiTFSI) significantly improves the conductivity of the dynamic network. (Figure 7c).[122] The dynamic imine exchange reaction of the prepared self-healing polyelectrolytes allows rapid structural or functional recovery and provides effective shape adaptation or configurability. Meanwhile, the SSE has excellent room temperature conductivity of 3.3×10^{-3} S cm^{-1}.

4.3.2. Covalent organic framework

COF is a three-dimensional framework material with regular pore channels formed by organic units interconnected by covalent bonds.[118] Niu et al. reported crystal covalent organic framework (COFs) to regulate the ion-directed migration channel and electrochemical window of solid electrolytes (Figure 7d).[123] The improved ionic conductivity is attributed to the overall orientation of the (001) crystalline planes in the COF structure, and the introduction of triazine and polyfluorophenyl broadens the electrochemical window by converting the imine bond into a more stable quinoline aromatic ring bond. According to DFT theory, the diffusion rate of Li^+ along covalent organic framework materials ($E_a = 0.43$ eV and $E_a = 0.40$ eV) is faster than that of Li^+ in the solid salt phase ($E_a = 0.62$ eV). COF is also used as the interface medium to improve the poor contact between lithium-metal electrode and electrolyte interface.[160]

To sum up, MOF and COF are introduced in the polymer matrix to prepare high-performance composite SSEs, which possess some unique structural advantages such as three-dimensional ion transport networks and flexibility. The organic framework has more possibilities in structural design through

carbon, silane, and boron atoms to manipulate their physicochemical properties. However, their practical application still has limitations, such as many complex interface effects, limited ion transport capacity, difficult treatment of waste liquid after reaction, etc.

4.4. Lithium conduction mechanism in polymer-based composite solid-state-electrolyte

4.4.1. Lewis acid-base interaction

Lewis acid-base theory exists between the anion acceptor (Lewis acid) and the electron donor (Lewis base), such as hydrogen-bond interaction, positive vacancy-salt interaction, and dipole-dipole interaction.[124] According to Lewis acid-base theory, the anion acceptor is a neutral molecule that can effectively immobilize the anion movement in lithium salts. It is a pair of electron acceptors, while the anions of lithium salts are essentially a pair of electron donors.

The inorganic filler has a Lewis acid center, which introduces the Lewis base into the polymer chain to form a complex interaction.[125] The Lewis acid center has a strong affinity for the anion and readily forms coordination.[10,126] Lewis acid groups on the surface of inorganic particles also form coordination with lithium salts, leading to higher-order dissociation of lithium salts and increasing the concentration of free Li^+. Therefore, fillers with Lewis acid centers form coordination interactions with polymers, which is considered a promising candidate strategy to improve the conductivity of solid electrolytes. Conduction path of composite electrolyte, (1) Fast ion conduction between ceramics; (2) Slow conduction between ceramics and polymers. Therefore, it helps increase the ionic conductivity of the polymer-based electrolyte by increasing the content of ceramics in a polymer matrix, designing 3d-structured ceramics, or constructing fast ion channels between polymer and ceramics.

Lewis acid-base interactions can effectively improve electrical conductivity, modulate the ionic conductivity of polymer electrolytes, and optimize the synergistic stiffness/flexibility dynamics between polymer nanoparticles. Hu and his colleagues creatively produced PEO and SiO_2 composite solid electrolytes through strong Lewis acid-base interaction and weak hydrogen bonds (Figure 8a).[127] The synergistic effects of

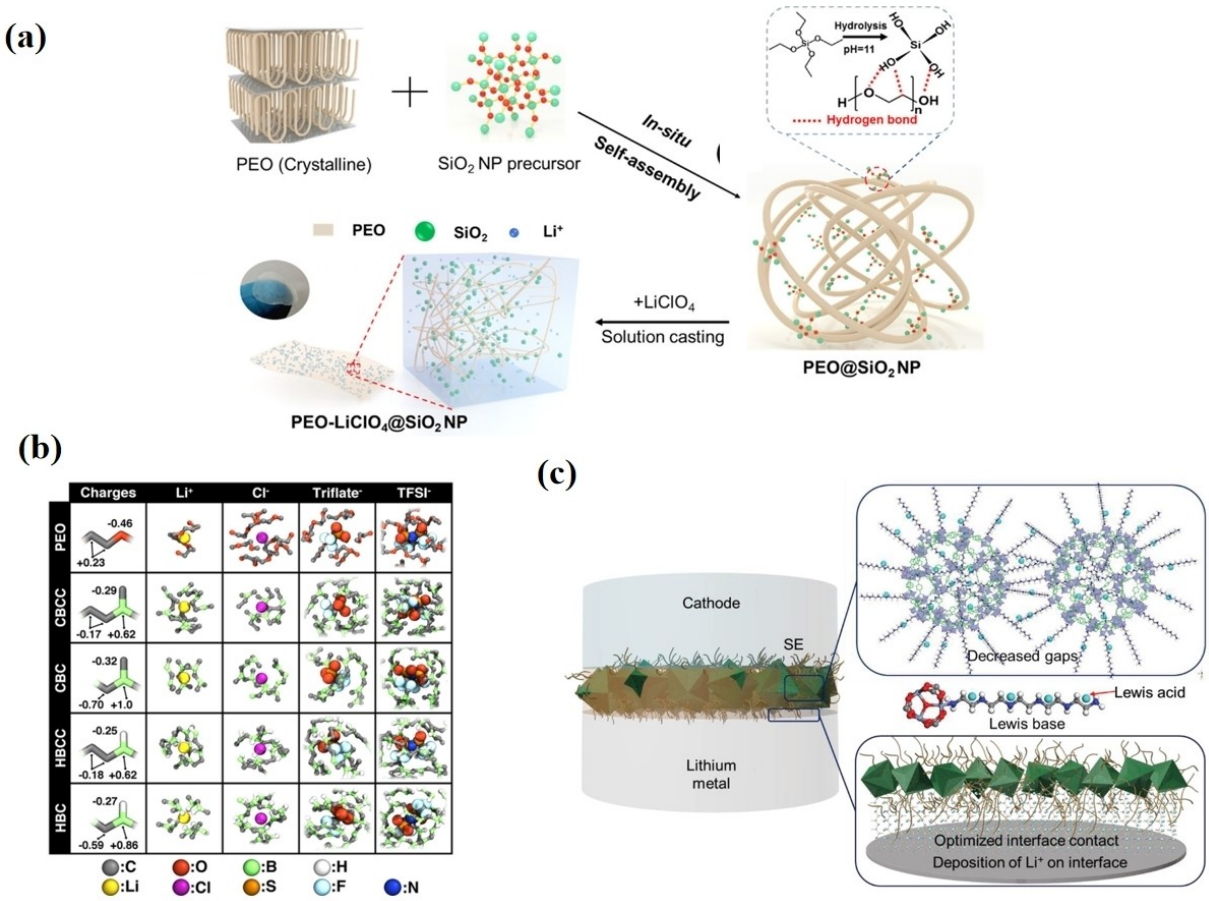

Figure 8. a) Lewis acid-base interaction of SiO_2 and PEO-based polymers. Adapted with permission from Ref. [127]. Copyright (2020) American Chemical Society. b) Contrasting ion coordination behavior in Lewis-basic and Lewis-acidic polymers, and histograms of the number of polymer-ion contacts averaged across the simulations. Adapted with permission from Ref. [130]. Copyright (2017) American Chemical Society. c) The molecular-scale interface engineering strategy of MOF with long chain Lewis base. Adapted with permission from Ref. [131]. Copyright (2020) Wiley-VCH GmbH.

SiO_2 filler and PEO through Lewis and hydrogen bonding interactions are as follows: 1) The –OH at the end of PEO will chemically interact with SiO_2 nanoparticles and lithium salts to reduce the crystallinity of PEO; 2) Enhanced molecular binding between SiO_2 nanoparticles and PEO molecular chains; 3) The hydrogen bonds between SiO_2 and PEO suppress the deformation of polymer chains, which facilitates the mechanical properties of SSE.[7] Based on the Lewis acid-base interaction of oxides, Xu et al. extracted CaO from eggshells as a strong Lewis alkaline filler compounding with PEO polymers.[128] The results showed that calcium oxide filler has superior ionic conductivity and a synergistic effect on PEO polymer chains. Wang et al. prepared a strong Lewis acid AlF_3compound with PEO form composite SSE.[129] Compared with the pure PEO-based SSE(6×10^{-4} S cm^{-1} at 60 °C, 550 h at 0.2 mA cm^{-2}), the ionic conductivity and Li metal stability were significantly improved (1.2×10^{-3} S cm^{-1}, over 3600 h).

Lewis base is chemically anchored to the open metal sites (OMSs) of MOF candidates, which can interact with Li^+ (Lewis acid). The stretched Lewis base long molecular chain is expected to minimize the ion transport gap between crystals and improve the contact. According to molecular dynamics simulations, Brett M. Savoie et al. found that Lewis acidic polyborane exhibits good Li^+ conductivity and lithium salt dissociation and has a larger lithium-ion mobility number than pure PEO. (Figure 8b).[130] In terms of experiments, many works have been done on the molecular design of Lewis acid-base-centered composite SSE, especially on advanced synthetic strategies for metal-organic frameworks. Li et al. successfully prepared Lewis base MOF-polymer composite SSE by decorating Lewis bases on the open metal sites of MOF molecules (Figure 8c).[131] Lewis acid-base interaction promotes Li^+ transition and transport. The Lewis base molecules are elongated and the ion transport gap between the crystals is reduced, which helps Li^+ transport between the crystal gaps and improves the electrode-electrolyte contact. In addition, it simultaneously improved the electrical conductivity and mechanical strength of PEO, and a strategy to introduce a bifunctional additive was proposed. Zeng et al. explored a solution-casting method that introduction of bifunctional additive zinc bis(2-ethyl-hexanoate) ($Zn(BEH)_2$) simultaneously improved the ionic conductivity and the inhibition of lithium dendrites.[132] The Lewis acid-base interaction between $Zn(BEH)_2$ and the PEO chain can successfully reduce the crystallinity of PEO and weaken the O–Li^+ interaction.

4.4.2. Vacancy

Oxygen ion vacancies in crystals tend to move through three mechanisms: direct migration, incomplete occupation, and coordinated migration, based on the classical crystal chemistry theory.[133] Li^+ vacancies are usually generated in the lattice of inorganic fillers. In general, the active inorganic filler deviates from the original chemical ratio, and oxygen vacancies appear in the lattice, leading to a large accumulation of Li+ on the surface and ion redistribution, and formation of a space charge layer, thus promoting the conductivity of the electrolyte.[103,134,135]

Considerable efforts have been made to introduce oxide inorganic fillers into polymers to obtain oxygen ion vacancies to improve their overall electrochemical properties. The Cui group prepared a Y_2O_3-doped ZrO_2 nanowire by electrospinning, which needs to be further compounded with PAN–$LiClO_4$ to obtain a solid electrolyte Y_2O_3 doping process with low valence metal ions leading to a high concentration of oxygen vacancies in ZrO_2, and the generated oxygen vacancies can also be used as Lewis acid sites in composite electrolytes (Figure 9a).[136] The obtained electrolyte increased the room temperature conductivity from 3.65×10^{-7} S cm^{-1} to 1.07×10^{-5} S cm^{-1}. Doping of low valence ions into high valence metal oxides is also a strategy to introduce vacancies for SSEs. Chen et al. demonstrated the direct introduction of oxygen vacancies into SSEs using Ca-doped CeO_2 nanotubes as inorganic fillers and polyethylene oxide (PEO)–LiTFSI as a substrate (Figure 9b).[137] The oxygen vacancy filler incorporated with PEO formed SSE significantly improved electrochemical performance($LiFePO_4$/Li battery 170 mAh g^{-1} at 0.2 C). The source of the increased discharge-specific capacity was investigated by DFT calculations. The oxygen vacancies on the surface of Ca–CeO_2 nanotubes interact with the anionic fraction ($TFSI^-$) of the lithium salt after the incorporation of PEO, which promotes the dissociation of the lithium salt, and the faster interfacial kinetic transport results in a small interfacial transfer resistance during charging and discharging.

Similarly, Guo et al. reported a PEO-based composite solid electrolyte coated with dopamine on the surface of LLZO particles showing good electrochemical properties with a room temperature conductivity of 1.15×10^{-4} S cm^{-1} (Figure 9c).[138] By analyzing the Fourier transform infrared spectra (FTIR), it was found that polydopamine (PDA) had characteristic peaks at 3550 cm^{-1} and Li_2CO_3 peaks at 1438 and 863 cm^{-1} after weak alkali treatment. Specifically, Li_2CO_3 contaminants on LLZTO particles can be transformed into a uniform PDA layer with a ~15 nm thickness by dopamine-induced polymerization. Compared with the untreated LLZTO, the PDA layer surface produces a space charge layer caused by lithium vacancies and lithium-ion redistribution, which promotes enhanced lithium ion transport in the composite electrolyte.

Briefly, the introduction of oxygen vacancies redistributes lithium ions on the surface of the inorganic filler, thus building a space charge layer to facilitate ion transport in the electrolyte. Theoretical developments in crystal chemistry can help to deepen our understanding with regard to the regulation of conductivity by inorganic fillers in terms of doping and morphology modulation. However, precise tuning of doping methods and vacancy concentrations remains a challenge. In addition, doping usually causes changes in the crystal space group, which inhibits the lithium transition. A clear understanding and appreciation of dopant ions are important for small changes in the crystal structure, but this remains a challenge.

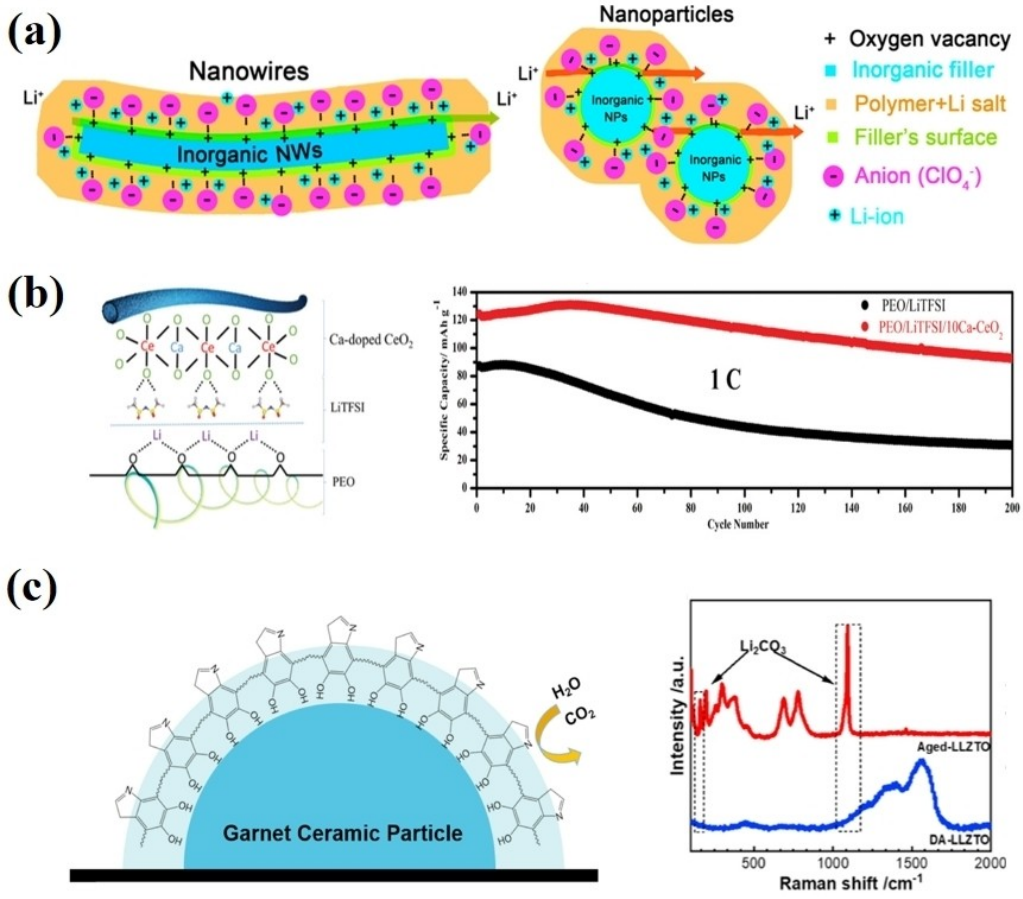

Figure 9. a) Lithium-ion transport in composite polymer electrolyte with nanowire filler. The positively charged oxygen vacancies on the filler surface strongly interact with anions and release lithium ions. Adapted with permission from Ref. [136]. Copyright (2016) American Chemical Society. b) Vacancy generation in Ca dope CeO_2 nanotubes enhances lithium ion transport in PEO-based electrolytes and full battery cycle performance. Adapted with permission from Ref. [137]. Copyright (2020) WILEY-VCH Verlag GmbH & Co. KGaA, Weinheim. c) Air-stable DA-treated garnet ceramic particles, and FTIR spectrum evidence. Adapted with permission from Ref. [138]. Copyright (2020) Elsevier B.V.

5. Interface Stability in Solid-State Electrolytes and Electrodes

5.1. High-voltage compatibility of polymer-based electrolyte, and interface modification

The "electrolyte window" is determined by the highest occupied molecular orbital (HOMO) and the lowest unoccupied orbital (LUMO). The cathode material is in a strongly oxidized state during the de-intercalation of lithium. Cathode potential (μ_c) can be shifted down to a state lower than the HOMO of SPE, leading to interfacial parasitic reactions.[10] When thermodynamically unstable at high voltages, the solid electrolyte decomposes to produce byproducts, which affect the ionic conductivity of the entire battery system. The decomposition of active components in the electrolyte caused by oxidation/reduction reactions during charge-discharge affects the electrochemical performance of the battery. Therefore, widening the electrochemical window of the solid electrolyte is very important to achieve high-specific-energy batteries.

Inorganic oxides have a wider electrochemical window, which is applicable for extending the electrochemical window of polymer-based solid electrolytes. For example, LLZNO incorporated PEO as a representative organic-inorganic composite solid electrolyte to extend the electrochemical window (Figure 10a).[139] Nd-doped LLZO has an electrochemical window of ~6 V, and the solid-state electrolyte compounded with PEO broadened the electrochemical window to 5.2 V. Similarly, Salian et al. prepared TiO_2 nanorod doped PMMA crosslinks PEG solid electrolyte, in which the stability of electrochemical performance is attributed to the electrodeposition of TiO_2 on the interface.[140] Supramolecular interactions between lithium salts and polymers, and hydrogen bonding between lithium salts and hydrogen atoms in the polymer backbone, have a positive impact on stabilizing high-voltage cathode (e.g., LCO, NCM, LNMO, etc.) interfaces. In addition, structural defects, energy disorders, and interface impurities of cathode materials may also affect the electrochemical window.[141]

Types of lithium salts and polymer matrix with different main chains and functional groups also affect the electrochemical window of solid electrolytes.[142] Lithium bis(oxalate)borate (LiDFOB) is a good lithium salt that promotes oxidation-resistant and low-resistance electrode/electrolyte interface layer. The relationship between poly (ethylene-glycol)

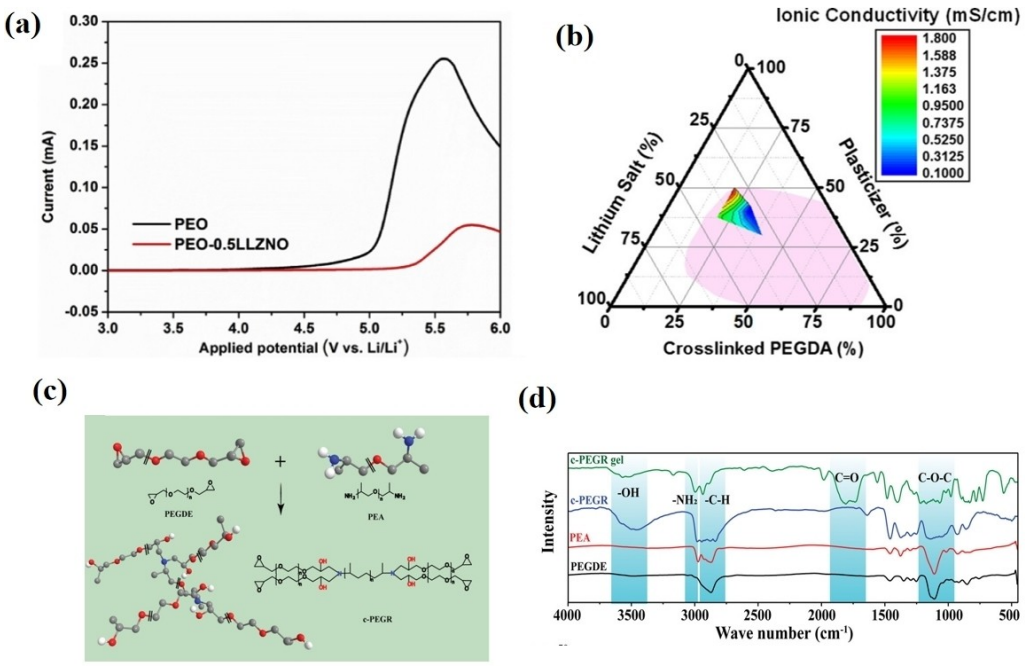

Figure 10. a) Inorganic filler LLZNO extends the electrochemical window of PEO-based solid electrolytes. Adapted with permission from Ref. [139]. Copyright (2019) WILEY-VCH Verlag GmbH & Co. KGaA, Weinheim. b) Ternary phase diagram of ionic conductivity crosslinking degree lithium salt content. Adapted with permission from Ref. [143]. Copyright (2018) American Chemical Society. c) Schematic of the synthesis and d) FITR diagram. Adapted with permission from Ref. [144]. Copyright (2021) The Authors. Advanced Science published by Wiley-VCH GmbH.

diacrylate (PEGDA) as a matrix and an electrochemical window in solid electrolytes is shown in Figure 10(b).[143] They found that LiDFOB crosslinked with PEGDA has a synergistic stabilizing effect on the high-voltage cathode, for which its electrochemical window can reach 4 V. The Sun group found that the electrochemical window of PEO-based electrolytes may be limited by the –OH functional group at the terminal group. The polyethylene glycol (PEG) and poly (ethylene glycol) dimethyl ether (PEGDME) have the same main chain, and the end groups are –OH and $–OCH_3$ respectively.[31] The –OH terminal group will be oxidized to –COOH (Li) and Li_2O at 4.05–4.3 V. When the voltage is increased above 4.3 V, the ether chain (–C–O–C–) in the polymer will be further oxidized. Based on this theory, Fang confined hydroxyl groups to the backbone of cross-linked polyethylene glycol resin (c–PEGR), which increased the oxidation potential of PEG-based polymeric materials to 4.36 V. (Figure 10c, d).[144]

For the electrochemical window of SSE, a variety of composite electrolytes are usually used to replace the single electrolyte. Heterogeneous layer structure electrolyte films with different compositions contact different electrode interfaces, allowing the cathode side to contact the oxidation-resistant electrolyte and the lithium metal side to contact the reduction-resistant electrolyte, which provides the opportunity to extend the electrochemical window of SSEs in a targeted manner. Luo and colleagues solidified PAN and PEO polymer electrolytes on the vermiculite nanowires framework.[145] PAN, PEGMA, and PEGDME can effectively suppress the dissolution of transition metal ions. PAN with a C≡N group is a rigid functional group with a lower energy level and better tolerance to oxidation reactions. The sandwich layer structure was synthesized as an emerging multilayer SSE membrane.[146–148]

5.2. Strategies to address Li-metal interfacial challenges

Lithium metal has a strong reducing property. When the process of charge-discharge, if the local current is distributed unevenly, dendrites would be produced on the surface of lithium metal and expand further along the grain boundaries, eventually leading to battery failure and diving.[8,149,150] In general, there are two ways to improve the lithium-metal interface stability as follows: 1) Modificating treatment at the lithium-metal interface to solve the problem of uneven local current distribution and inhibit the nucleation of lithium dendrites. 2) Improving the mechanical properties of the SSE to suppress the growth of lithium dendrites and the extension of cracks in the SSE.

Considerable efforts have been made to solve the local uneven current density distribution at the interface. Fan et al. demonstrated a method of inserting polyethylene carbonate (PEC) polymer into the interlayer of single ion conductor Lithium Montmorillonite (LiMNT), using the synergistic effect of intercalated electrolyte and a three-dimensional lithium anode with fluoroethylene carbonate (FEC) solvent and poly (tetrafluoroethylene) (PTFE) adhesive, solid-state lithium battery with stable Li^+ electrodeposited solid electrolyte and 3D Li composite anode (Figure 11a).[151] Li symmetric battery can stably cycle over 600 h at 0.5 mA cm^{-2}. The addition of a buffer layer is also a strategy to improve the point-to-point contact at

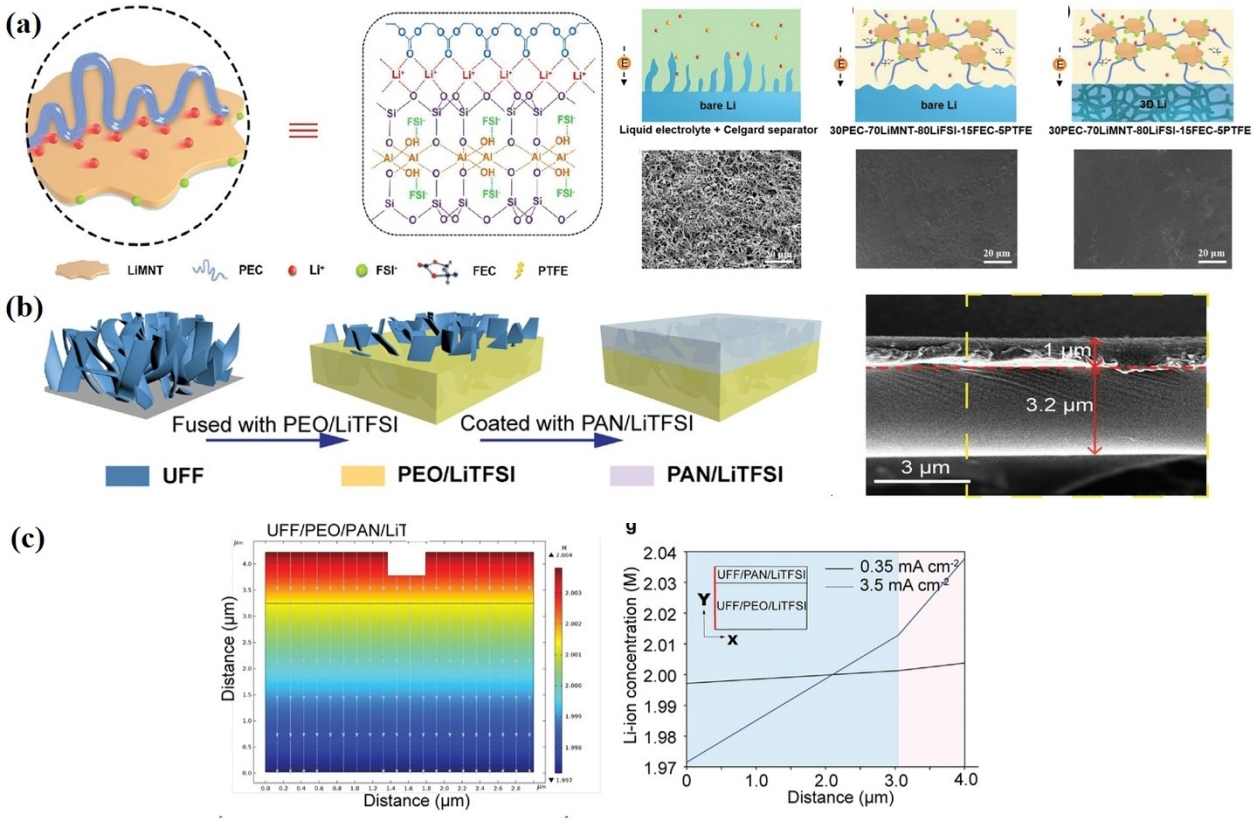

Figure 11. a) PEC–LiMNT–CSE enhances ion transfer and optimizes Li^+ deposition. Adapted with permission from Ref. [151]. Copyright (2019) WILE-VCH. b) Cross-sectional SEM image of the as-spun Vermiculite nanofibers (UFF). c) Simulation of Li-ion gradient in the UFF/PEO/PAN/LiTFSI SSE, and Li-ion concentration along the *Y* axis in the SSE. Adapted with permission from Ref. [145]. Copyright (2021) Wiley-VCH.

the lithium metal and LAGP electrolyte interface, thereby inhibiting the growth of lithium dendrites.[152]

The selection of high flux materials to improve the mechanical properties and interfacial contacts is important to suppress the cell failure caused by further Li dendrite expansion (Figure 11b, c).[145] Chen and his colleagues report an asymmetric solid electrolyte film with very good mechanical properties Young's modulus of 659.7 MPa. And the lithium metal-contacting side is smooth, ensuring a uniform current density distribution (Figure 11d).[112] However, introducing LATP or LAGP as a skeleton on the lithium metal interface side to increase the mechanical strength is also a strategy to inhibit the growth and penetration of lithium dendrites. Li et al. built a soft surface by coating LATP on the surface of PE film and backfilling PEO/LiTFSI, in which the tensile strength of the film is up to 9 MPa. The composite solid electrolytic membrane has an excellent effect of inhibiting lithium dendrite, and can stably cycle for more than 2000 h under the polarization current of 0.2 mA cm^{-2}. Based on these considerations, the construction of a specific solid electrolyte interface or the introduction of a skeleton to increase the mechanical strength of the membrane is expected to inhibit the growth and crack propagation of lithium dendrites and secure solid-state battery applications.

6. All-Solid-State Battery Industrialization and New Technologies

The solid electrolyte film acts intuitively as both a separator for the positive and negative electrodes, and it can also typically be cast onto the electrode surface either by a film formation process or by direct coating. Based on a "roll-to-roll" process, the development in terms of industrialization, battery failure mechanisms, and models predicts new electrolyte materials of the fabrication of SSBs cannot be ignored.

In recent years, BMW, Ford, Hyundai, and other automobile enterprises have successively invested in solid-state battery products. Toyota and Volkswagen plan to build and load solid-state lithium battery production lines for electric vehicles in 2028 and 2025. However, the industrialization of solid-state lithium batteries still faces problems, including high production costs, a narrow range of working temperatures, ceramic with air sensitivity and so on.[153] Meanwhile, the recycling of electrode/electrolyte materials from lithium batteries is also significant for SSBs commercialization and sustainable development, which is mainly carried out through the combination of various metallurgical methods after the disassembly and pretreatment of lithium batteries.[154] Avoiding contamination of components is one of the technical challenges during battery disassembly and recycling.[155]

"Machine learning" artificial intelligence techniques are expected to accelerate the development of solid-state battery systems and materials, and guide researchers in the rational design of advanced solid-state electrolytes. The team at Tsinghua University has proposed a comprehensive hierarchical Bayesian model and an early life prediction model that requires only a small number of samples and cycle data to accurately predict and evaluate the fast charging performance of batteries.[156] To better reveal the relationship between the thickness and performance of solid electrolyte films, Chen and his colleagues analyzed the multivariate interdependence between performance and experimental parameters through a combination of machine learning and statistical methods, and experimentally verified the optimal preparation parameters and obtained thin solid electrolyte films with good performance.[157]

Simulations and first-principles calculations are tools to better explain the operating mechanisms in solid-state batteries. Cui et al. proved through electric field simulation that isolated lithium highly corresponds to battery operation. Rapid discharge can promote the recovery of isolated lithium to anode growth.[158] Wang et al. simulated the evolution of Li^+ concentration near the lithium mental surface by finite element analysis.[159] It verified that the COF–SSE can adjust the lithium-ion flux and induce the current density to be evenly distributed on the anode surface, which makes Li^+ deposited uniformly. In addition, Shi et al. conducted a comprehensive and detailed review of the application of simulation methods.[160] It summarized three aspects: ion diffusion, stress evolution, and electrodeposition, according to the existing work of phase field simulation in rechargeable batteries.

For the solid-state electrolyte which is faced with the joint influence of many parameters, we highly recommend screening appropriate groups of parameters through the machine learning method to improve efficiency. Considering that the interface problems are difficult to be characterized directly at present, the simulation technology is selected to rationalize the problems of the battery and provide directions for further solutions.

7. Summary and Outlook

Polymer has a large number of functional groups, better flexibility and interfacial wettability as one of the candidate materials for SSE. Its composites can form various ion-conducting channels and form tight contacts with electrodes. These properties are of great importance for the development of high-specific energy all-solid-state batteries. Here, we discuss and review the latest research advances in polymer-based solid-state electrolytes focusing on four aspects: First, we summarize the various functional groups and valence bonds of the main polymeric materials used in solid electrolytes and illustrate the dynamic mechanisms of ions in solid electrolytes. Additionally, based on recent research advances, we discuss solid composite electrolytes with ceramic fillers combined with polymers. Then, we focused on the interfacial modification strategies of polymer-based electrolytes to stabilize the high-voltage cathode interface and suppress lithium metal dendrites. The layout of the industrialization of solid-state batteries, machine learning to develop new solid-state electrolyte materials, and simulation-assisted elaboration of electrochemical mechanisms are the future development of SSEs to be considered.

Although numerous efforts have been put on polymer-based electrolytes, some unfathomable mechanisms and materials issues remain unsolved, which impede the practical application of solid electrolytes in high energy density solid-state lithium metal batteries:

1. Development of polymer-based solid electrolytes with high room temperature conductivity. The function of the electrolyte is to transport lithium ions between positive and negative active material particle surfaces. The conductivity of most polymer and organic-inorganic composite electrolytes can only reach about 10^{-4} S cm^{-1} at room temperature. There is still a gap with the room temperature conductivity of 10^{-2}–10^{-3} S cm^{-1} for conventional liquid electrolytes. This paper elucidates the influence of functional groups and structural design of electrolytes on room temperature conductivity, and also needs to pay attention to the interaction between residual solvents and electrolytes in electrolytes, and electrode materials, which may affect the ionic conductivity during charging and discharging.
2. Develop oxidation-resistant polymer-based electrolytes to build stable cathode electrode-electrolyte interfaces. The electrode and electrolyte may decompose to form new compounds, and such compounds can affect the ion transport at the interface and form a large interfacial transfer resistance. Polymer molecular structure modification, multilayer structure, high-voltage cathode coating and other modification strategies are necessary to develop solid-state batteries with a stable high-voltage cathode-electrolyte interface.
3. Inhibition of inhomogeneous deposition of lithium ions, penetration of dendritic crystals and crack growth at the lithium-metal interface. Currently, the formation mechanism of SEI is based on the understanding of lithium dendrites in liquid electrolytes. There are differences in the lithium-metal interface with SSE. There is the basis for solving the interfacial stability of lithium metal-SSE that the nucleation of lithium metal, the growth of lithium dendrites and the propagation of lithium dendrite cracks in SSE. The formation and expansion of lithium dendrites should not only consider the electrochemical kinetic processes but also pay attention to the mechanical properties of the solid-state electrolyte.
4. Develop advanced, dynamic, and finer electrochemical characterization methods. Given the important role of electrode materials and interfaces on battery performance, the changes in phase and ionic valence bonds of electrode materials during cycling were studied by physical and chemical methods such as Fourier transform infrared spectroscopy (FTIR), X-ray photoelectron spectroscopy (XPS), X-ray energy spectroscopy (XRD). The morphology of electrode particles was observed by scanning electron

microscope (SEM) and projection electron microscope (TEM). However, current characterization methods are still limited for materials with air sensitivity and irradiation sensitivity. Real-time observation of microstructural changes, crystal structure and phase changes in the bulk remains a challenge. The development of advanced electrode material characterization technology enables it to observe the changes of phase and micromorphology of electrode batteries in real time, establish the relationship between parameter phase micromorphology, and establish the structure-activity relationship between characterization and electrochemical properties, which is a necessary condition to improve the understanding of electrode materials of solid-state battery. Current characterization methods still fail to observe the composition and structural changes of the interface in situ. DFT and molecular dynamics and force field simulation (COMSOL) are also pioneering methods to clarify the ion transport process of electrode and electrolyte materials and the basis of interfacial instability.

5. Control of the coupling relationship between electrolyte membrane thickness and conductivity. The thickness of the solid electrolyte membrane is inversely proportional to the conductivity and affects the internal resistance and energy density of the all-solid-state battery. However, there is a tension between minimizing electrolyte film thickness and mechanical strength. The thickness of the electrolyte film in solid-state batteries is a challenge for both conductivity and safety. In addition, during charge-discharge cycles, electrolyte components need to be considered to react and be consumed at the positive and negative electrodes, resulting in a reduction in thickness.
6. The physical properties and processing technology of SSE membranes are also worthy of attention. The mechanical properties and thermal stability of polymer-based materials are poor. Current research strategies focus on introducing polymers with rigid bonds to improve their mechanical properties. However, with the development of electrolyte thin membranes, it is difficult to take both ultra-thin and mechanical properties into account. In terms of thermal stability, some studies have added additive flame retardants into polymer electrolyte membranes, it is also a feasible direction. In addition, solid electrolytes and solid-state batteries are mostly limited to small button cells, which cannot satisfy the producibility and flexibility requirements of diversified energy storage devices.
7. The price, environmental friendliness, and future battery recycling of solid-state batteries. According to the different requirements of practical application, various solid-state batteries are being developed. Sodium ion solid-state batteries and potassium ion solid-state batteries are also considered supplements. Some basic theories and strategies of lithium mental SSB can be applied to other battery systems to avoid wasteful duplication of effort. Large-scale production should take into account the cost, toxicity, long-term storage stability and environmental friendliness of organic polymers and solvents. After the batteries are scrapped, we should also consider the recycling of battery materials and the disposal of waste materials.

In summary, the rapid development of polymer-based solid electrolyte materials has confirmed the feasibility of sustainable, safe, and efficient energy storage through solid-state batteries. The vigorous development of novel solid electrolytes and their interface engineering provides more choices for the practical application of lithium-ion solid-state batteries under various conditions. It is expected that the continuous development of solid electrolyte materials will bring new opportunities for the green and sustainable development of the next generation of solid-state lithium metal batteries and other energy storage materials.

Acknowledgements

Financial supports from National Key Research and Development Program of China (SQ2022YFB3800005) and National Natural Scientific Foundation of China (U21A2080) and Beijing Natural Science Foundation (Z200011) are gratefully acknowledged.

Conflict of Interest

The authors declare no conflict of interest.

Keywords: all-solid-state batteries · composite solid electrolytes · ion conductivity · interface stability · polymer solid electrolytes

[1] M. Winter, B. Barnett, K. Xu, *Chem. Rev.* **2018**, *118*, 11433–11456.
[2] Y. Zhao, L. Wang, Y. Zhou, Z. Liang, N. Tavajohi, B. Li, T. Li, *Adv. Sci.* **2021**, *8*, 2198–3844.
[3] M. S. Whittingham, *Chem. Rev.* **2014**, *114*, 11414–11443.
[4] J. B. Goodenough, Y. Kim, *Chem. Mater.* **2010**, *22*, 587–603.
[5] A. Manthiram, Y. Fu, Y.-S. Su, *Acc. Chem. Res.* **2013**, *46*, 1125–1134.
[6] P. G. Bruce, S. A. Freunberger, L. J. Hardwick, J.-M. Tarascon, *Nat. Mater.* **2012**, *11*, 19–29.
[7] J. Wan, J. Xie, D. G. Mackanic, W. Burke, Z. Bao, Y. Cui, *Mater. Today Nano* **2018**, *4*, 1–16.
[8] Y. Xiao, Y. Wang, S.-H. Bo, J. C. Kim, L. J. Miara, G. Ceder, *Nat. Rev. Mater.* **2020**, *5*, 105–126.
[9] W. Zhou, S. Wang, Y. Li, S. Xin, A. Manthiram, J. B. Goodenough, *J. Am. Chem. Soc.* **2016**, *138*, 9385–9388.
[10] Q. Zhou, J. Ma, S. Dong, X. Li, G. Cui, *Adv. Mater.* **2019**, *31*, 1521–4095.
[11] Y. Zheng, Y. Yao, J. Ou, M. Li, D. Luo, H. Dou, Z. Li, K. Amine, A. Yu, Z. Chen, *Chem. Soc. Rev.* **2020**, *49*, 8790–8839.
[12] D. Zhou, D. Shanmukaraj, A. Tkacheva, M. Armand, G. Wang, *Chem* **2019**, *5*, 2326–2352.
[13] Y. Guo, S. Wu, Y.-B. He, F. Kang, L. Chen, H. Li, Q.-H. Yang, *eScience* **2022**, *2*, 138–163.
[14] H. Zhang, L. Huang, H. Xu, X. Zhang, Z. Chen, C. Gao, C. Lu, Z. Liu, M. Jiang, G. Cui, *eScience* **2022**, *2*, 201–208.
[15] Y. Chen, Z. Wang, X. Li, X. Yao, C. Wang, Y. Li, W. Xue, D. Yu, S. Y. Kim, F. Yang, A. Kushima, G. Zhang, H. Huang, N. Wu, Y.-W. Mai, J. B. Goodenough, J. Li, *Nature* **2020**, *578*, 251–255.
[16] Y. Liu, Y. Zhao, W. Lu, L. Sun, L. Lin, M. Zheng, X. Sun, H. Xie, *Nano Energy* **2021**, *88*, 2211–2855.
[17] Q.-T. Pham, Y.-H. Jheng, D.-S. Tsai, J.-Y. Lai, C.-C. Hu, C.-S. Chern, *J. Appl. Polym. Sci.* **2022**, *139*, e52158.
[18] Y. Wu, Y. Li, Y. Wang, Q. Liu, Q. Chen, M. Chen, *J. Energy Chem.* **2022**, *64*, 62–84.

[19] B. Tang, Q. Zhou, X. Du, J. Zhang, H. Zhang, Z. Zou, X. Zhou, G. Cui, *Nano Sel.* **2020**, *1*, 59–78.
[20] B. Xu, X. Li, C. Yang, Y. Li, N. S. Grundish, P.-H. Chien, K. Dong, I. Manke, R. Fang, N. Wu, H. Xu, A. Dolocan, J. B. Goodenough, *J. Am. Chem. Soc.* **2021**, *143*, 6542–6550.
[21] C. Song, Z. Li, J. Peng, X. Wu, H. Peng, S. Zhou, Y. Qiao, H. Sun, L. Huang, S.-G. Sun, *J. Mater. Chem. A* **2022**, *10*, 16087–16094.
[22] C. M. Septani, O. Shih, Y.-Q. Yeh, Y.-S. Sun, *Langmuir* **2022**, *38*, 5987–5995.
[23] M. Chintapalli, T. N. P. Le, N. R. Venkatesan, N. G. Mackay, A. A. Rojas, J. L. Thelen, X. C. Chen, D. Devaux, N. P. Balsara, *Macromolecules* **2016**, *49*, 1770–1780.
[24] R. Bouchet, T. N. T. Phan, E. Beaudoin, D. Devaux, P. Davidson, D. Bertin, R. Denoyel, *Macromolecules* **2014**, *47*, 2659–2665.
[25] D. Sharon, P. Bennington, M. A. Webb, C. Deng, J. J. de Pablo, S. N. Patel, P. F. Nealey, *J. Am. Chem. Soc.* **2021**, *143*, 3180–3190.
[26] S. Pal, R. K. Srivastava, B. Nandan, *Polymer* **2021**, *231*, 124119.
[27] Y. Ugata, M. L. Thomas, T. Mandai, K. Ueno, K. Dokko, M. Watanabe, *Phys. Chem. Chem. Phys.* **2019**, *21*, 9759–9768.
[28] L. Ran, M. Li, E. Cooper, B. Luo, I. Gentle, L. Wang, R. Knibbe, *Energy Storage Mater.* **2021**, *41*, 8–13.
[29] Z. Lu, L. Peng, Y. Rong, E. Wang, R. Shi, H. Yang, Y. Xu, R. Yang, J. Chao, *ENERGY Environ. Mater.* **2022**, DOI 10.1002/eem2.12498.
[30] K. He, S. H.-S. Cheng, J. Hu, Y. Zhang, H. Yang, Y. Liu, W. Liao, D. Chen, C. Liao, X. Cheng, Z. Lu, J. He, J. Tang, R. K. Y. Li, C. Liu, *Angew. Chem. Int. Ed.* **2021**, *60*, 12116–12123; *Angew. Chem.* **2021**, *133*, 12223–12230.
[31] X. Yang, M. Jiang, X. Gao, D. Bao, Q. Sun, N. Holmes, H. Duan, S. Mukherjee, K. Adair, C. Zhao, J. Liang, W. Li, J. Li, Y. Liu, H. Huang, L. Zhang, S. Lu, Q. Lu, R. Li, C. V. Singh, X. Sun, *Energy Environ. Sci.* **2020**, *13*, 1318–1325.
[32] B. Zhou, D. He, J. Hu, Y. Ye, H. Peng, X. Zhou, X. Xie, Z. Xue, *J. Mater. Chem. A* **2018**, *6*, 11725–11733.
[33] Z. Wang, L. Shen, S. Deng, P. Cui, X. Yao, *Adv. Mater.* **2021**, *33*, 2100353.
[34] H. Wang, J. Song, K. Zhang, Q. Fang, Y. Zuo, T. Yang, Y. Yang, C. Gao, X. Wang, Q. Pang, D. Xia, *Energy Environ. Sci.* **2022**, *15*, 5149–5158.
[35] Y.-J. Wang, D. Kim, *J. Power Sources* **2007**, *166*, 202–210.
[36] Y.-J. Wang, D. Kim, *J. Membr. Sci.* **2008**, *312*, 76–83.
[37] R. He, M. Echeverri, D. Ward, Y. Zhu, T. Kyu, *J. Membr. Sci.* **2016**, *498*, 208–217.
[38] R. He, T. Kyu, *Macromolecules* **2016**, *49*, 5637–5648.
[39] Y. Zhang, W. Feng, Y. Zhen, P. Zhao, X. Wang, L. Li, *Ionics* **2022**, *28*, 2751–2758.
[40] N. Meng, H. Zhang, S. Lianli, F. Lian, *J. Membr. Sci.* **2020**, *597*, 117768.
[41] Q. Wang, T. Dong, Q. Zhou, Z. Cui, X. Shangguan, C. Lu, Z. Lv, K. Chen, L. Huang, H. Zhang, G. Cui, *Sci. China Chem.* **2022**, *65*, 934–942.
[42] J.-E. Lee, J. Choi, D. J. Lee, S. Lee, H. G. Chae, *Carbon* **2022**, *191*, 515–524.
[43] J. Ramachandran, J. M. Serrano, T. Liu, J. Cho, P. J. Arias-Monje, M. Lu, M. H. Kirmani, J. Elliott, S. S. Jang, G. Liu, S. Kumar, *Carbon* **2022**, *192*, 332–346.
[44] C. He, J. Liu, J. Cui, J. Li, X. Wu, *Solid State Ionics* **2018**, *315*, 102–110.
[45] N. Meng, X. Zhu, F. Lian, *Particuology* **2022**, *60*, 14–36.
[46] D. Zhou, Y.-B. He, R. Liu, M. Liu, H. Du, B. Li, Q. Cai, Q.-H. Yang, F. Kang, *Adv. Energy Mater.* **2015**, *5*, 1500353.
[47] J. Ye, F. He, J. Nie, Y. Cao, H. Yang, X. Ai, *J. Mater. Chem. A* **2015**, *3*, 7406–7412.
[48] D. Zhang, X. Xu, S. Ji, Z. Wang, Z. Liu, J. Shen, R. Hu, J. Liu, M. Zhu, *ACS Appl. Mater. Interfaces* **2020**, *12*, 21586–21595.
[49] Z. Xiao, T. Long, L. Song, Y. Zheng, C. Wang, *Ionics* **2022**, *28*, 15–26.
[50] L.-Y. Yang, J.-H. Cao, B.-R. Cai, T. Liang, D.-Y. Wu, *Electrochim. Acta* **2021**, *382*, 138346.
[51] Z. Li, S. Wang, J. Shi, Y. Liu, S. Zheng, H. Zou, Y. Chen, W. Kuang, K. Ding, L. Chen, Y. Lan, Y. Cai, Q. Zheng, *Energy Storage Mater.* **2022**, *47*, 262–270.
[52] X. Wang, *Polymer* **2021**, *230*, 124038.
[53] W.-P. Chen, H. Duan, J.-L. Shi, Y. Qian, J. Wan, X.-D. Zhang, H. Sheng, B. Guan, R. Wen, Y.-X. Yin, S. Xin, Y.-G. Guo, L.-J. Wan, *J. Am. Chem. Soc.* **2021**, *143*, 5717–5726.
[54] S.-B. Son, T. Gao, S. P. Harvey, K. X. Steirer, A. Stokes, A. Norman, C. Wang, A. Cresce, K. Xu, C. Ban, *Nat. Chem.* **2018**, *10*, 532–539.
[55] W. Zhang, M. Sun, J. Yin, E. Abou-Hamad, U. Schwingenschlögl, P. M. F. J. Costa, H. N. Alshareef, *Angew. Chem. Int. Ed.* **2021**, *60*, 1355–1363; *Angew. Chem.* **2021**, *133*, 1375–1383.
[56] J. Wang, Q. Yuan, Z. Ren, C. Sun, J. Zhang, R. Wang, M. Qian, Q. Shi, R. Shao, D. Mu, Y. Su, J. Xie, F. Wu, G. Tan, *Nano Lett.* **2022**, *22*, 5221–5229.
[57] Y. Liang, H. Liu, G. Wang, C. Wang, D. Li, Y. Ni, L.-Z. Fan, *Adv. Energy Mater.* **2022**, *12*, 2201555.
[58] H. Jiang, X. Xu, Q. Guo, H. Wang, J. Zheng, Y. Zhu, H. Jiang, O. O. Kapitanova, V. S. Volkov, J. Wang, Y. Chen, Y. Wang, Y. Han, C. Zheng, K. Xie, S. Xiong, Y. Liu, X. Jiao, *J. Energy Chem.* **2022**, DOI 10.1016/j.jechem.2022.11.059.
[59] L.-Z. Fan, Y.-S. Hu, A. J. Bhattacharyya, J. Maier, *Adv. Funct. Mater.* **2007**, *17*, 2800–2807.
[60] S. Xu, Z. Sun, C. Sun, F. Li, K. Chen, Z. Zhang, G. Hou, H. Cheng, F. Li, *Adv. Funct. Mater.* **2020**, *30*, 2007172.
[61] C. M. Costa, M. M. Silva, S. Lanceros-Méndez, *RSC Adv.* **2013**, *3*, 11404.
[62] X. Zhang, J. Han, X. Niu, C. Xin, C. Xue, S. Wang, Y. Shen, L. Zhang, L. Li, C.-W. Nan, *Batteries & Supercaps* **2020**, *3*, 876–883.
[63] J. Chen, H. Zhang, H. Chen, E. Xia, Y. Wu, Z. Li, *J. Power Sources* **2022**, *548*, 232109.
[64] C.-Y. Tsai, Y.-L. Liu, *J. Membr. Sci.* **2022**, *651*, 120456.
[65] L. Cong, Y. Li, W. Lu, J. Jie, Y. Liu, L. Sun, H. Xie, *J. Power Sources* **2020**, *446*, 227365.
[66] Z. Li, Y. Lu, Q. Su, M. Wu, X. Que, H. Liu, *ACS Appl. Mater. Interfaces* **2022**, *14*, 5402–5413.
[67] Z. Yao, K. Zhu, X. Li, J. Zhang, J. Chen, J. Wang, K. Yan, J. Liu, *Electrochim. Acta* **2022**, *404*, 139769.
[68] J.-P. Zeng, J.-F. Liu, H.-D. Huang, S.-C. Shi, B.-H. Kang, C. Dai, L.-W. Zhang, Z.-C. Yan, F. J. Stadler, Y.-B. He, Y.-F. Huang, *J. Mater. Chem. A* **2022**, *10*, 18061–18069.
[69] Y.-F. Huang, T. Gu, G. Rui, P. Shi, W. Fu, L. Chen, X. Liu, J. Zeng, B. Kang, Z. Yan, F. J. Stadler, L. Zhu, F. Kang, Y.-B. He, *Energy Environ. Sci.* **2021**, *14*, 6021–6029.
[70] S. Liu, L. Zhou, J. Han, K. Wen, S. Guan, C. Xue, Z. Zhang, B. Xu, Y. Lin, Y. Shen, L. Li, C.-W. Nan, *Adv. Energy Mater.* **2022**, *12*, 2200660.
[71] A. Hosseinioun, P. Nürnberg, M. Schönhoff, D. Diddens, E. Paillard, *RSC Adv.* **2019**, *9*, 27574–27582.
[72] W. Wang, Y. Wang, W. Huang, M. Zhou, L. Lv, M. Shen, H. Zheng, *ACS Appl. Mater. Interfaces* **2021**, *13*, 6919–6929.
[73] D. Yang, L. He, Y. Liu, W. Yan, S. Liang, Y. Zhu, L. Fu, Y. Chen, Y. Wu, *J. Mater. Chem. A* **2019**, *7*, 13679–13686.
[74] Z. Zhou, Y. Feng, J. Wang, B. Liang, Y. Li, Z. Song, D. M. Itkis, J. Song, *Chem. Eng. J.* **2020**, *396*, 125254.
[75] C. Zhao, Q. Sun, J. Luo, J. Liang, Y. Liu, L. Zhang, J. Wang, S. Deng, X. Lin, X. Yang, H. Huang, S. Zhao, L. Zhang, S. Lu, X. Sun, *Chem. Mater.* **2020**, *32*, 10113–10119.
[76] Y. Ma, J. Wan, Y. Yang, Y. Ye, X. Xiao, D. T. Boyle, W. Burke, Z. Huang, H. Chen, Y. Cui, Z. Yu, S. T. Oyakhire, Y. Cui, *Adv. Energy Mater.* **2022**, *12*, 2103720.
[77] D. Chen, M. A. Mahmoud, J.-H. Wang, G. H. Waller, B. Zhao, C. Qu, M. A. El-Sayed, M. Liu, *Nano Lett.* **2019**, *19*, 2037–2043.
[78] D. Zhang, L. Zhang, K. Yang, H. Wang, C. Yu, D. Xu, B. Xu, L.-M. Wang, *ACS Appl. Mater. Interfaces* **2017**, *9*, 36886–36896.
[79] C. Sun, J. Liu, Y. Gong, D. P. Wilkinson, J. Zhang, *Nano Energy* **2017**, *33*, 363–386.
[80] J. Qiu, X. Liu, R. Chen, Q. Li, Y. Wang, P. Chen, L. Gan, S.-J. Lee, D. Nordlund, Y. Liu, X. Yu, X. Bai, H. Li, L. Chen, *Adv. Funct. Mater.* **2020**, *30*, 1909392.
[81] H. Liu, X.-B. Cheng, J.-Q. Huang, H. Yuan, Y. Lu, C. Yan, G.-L. Zhu, R. Xu, C.-Z. Zhao, L.-P. Hou, C. He, S. Kaskel, Q. Zhang, *ACS Energy Lett.* **2020**, *5*, 833–843.
[82] A. Manthiram, X. Yu, S. Wang, *Nat. Rev. Mater.* **2017**, *2*, 16103.
[83] C. Li, Y. Huang, X. Feng, Z. Zhang, H. Gao, J. Huang, *J. Colloid Interface Sci.* **2021**, *594*, 1–8.
[84] D. Lin, P. Y. Yuen, Y. Liu, W. Liu, N. Liu, R. H. Dauskardt, Y. Cui, *Adv. Mater.* **2018**, *30*, 1802661.
[85] C. Ma, J. Zhang, M. Xu, Q. Xia, J. Liu, S. Zhao, L. Chen, A. Pan, D. G. Ivey, W. Wei, *J. Power Sources* **2016**, *317*, 103–111.
[86] Y. He, Y. Li, Q. Tong, J. Zhang, J. Weng, M. Zhu, *ACS Appl. Mater. Interfaces* **2021**, *13*, 41593–41599.
[87] X. Zheng, T. Yang, J. Wei, C. Wang, M. Chen, *J. Power Sources* **2021**, *496*, 229843.
[88] J. Li, L. Zhu, J. Zhang, M. Jing, S. Yao, X. Shen, S. Li, F. Tu, *Int. J. Energy Res.* **2021**, *45*, 7663–7674.
[89] S. Liu, Y. Zhao, X. Li, J. Yu, J. Yan, B. Ding, *Adv. Mater.* **2021**, *33*, 2008084.

[90] Z. Zhang, YingHuang, G. Zhang, L. Chao, *Energy Storage Mater.* **2021**, *41*, 631–641.
[91] S. Li, J. Lu, Z. Geng, Y. Chen, X. Yu, M. He, H. Li, *ACS Appl. Mater. Interfaces* **2022**, *14*, 1195–1202.
[92] Y. Choo, D. M. Halat, I. Villaluenga, K. Timachova, N. P. Balsara, *Prog. Polym. Sci.* **2020**, *103*, 101220.
[93] E. Staunton, Y. G. Andreev, P. G. Bruce, *Faraday Discuss.* **2007**, *134*, 143–156.
[94] A. L. Monaca, W. Zhu, Z. Feng, G. Bertoni, D. Campanella, G. Girard, S. Savoie, A. G. Nita, D. Clement, H. Demers, A. Vijh, F. Rosei, A. Paolella, *J. Electrochem. Soc.* **2022**, *169*, 040515.
[95] S. Jayanthi, S. Shenbagavalli, M. Muthuvinayagam, B. Sundaresan, *Mater. Sci. Eng. B* **2022**, *285*, 115942.
[96] A. R. Polu, H.-W. Rhee, *J. Ind. Eng. Chem.* **2016**, *37*, 347–353.
[97] S. Cui, X. Wu, Y. Yang, M. Fei, S. Liu, G. Li, X.-P. Gao, *ACS Energy Lett.* **2022**, *7*, 42–52.
[98] K. Huang, Y. Wang, H. Mi, D. Ma, B. Yong, P. Zhang, *J. Mater. Chem. A* **2020**, *8*, 20593–20603.
[99] F. Chen, X. Wang, M. Armand, M. Forsyth, *Nat. Mater.* **2022**, *21*, 1175–1182.
[100] Y. Horowitz, M. Lifshitz, A. Greenbaum, Y. Feldman, S. Greenbaum, A. P. Sokolov, D. Golodnitsky, *J. Electrochem. Soc.* **2020**, *167*, 160514.
[101] Y. Dong, I.-W. Chen, J. Li, *Chem. Mater.* **2022**, *34*, 5749–5765.
[102] G. Cui, *Matter* **2020**, *2*, 805–815.
[103] C. Wang, K. Fu, S. P. Kammampata, D. W. McOwen, A. J. Samson, L. Zhang, G. T. Hitz, A. M. Nolan, E. D. Wachsman, Y. Mo, V. Thangadurai, L. Hu, *Chem. Rev.* **2020**, *120*, 4257–4300.
[104] J. Tang, L. Wang, C. Tian, C. Chen, T. Huang, L. Zeng, A. Yu, *ACS Appl. Mater. Interfaces* **2022**, *14*, 4170–4178.
[105] M. Lei, *Energy Storage Mater.* **2022**, *47*, 551–560.
[106] E. J. Cussen, *J. Mater. Chem.* **2010**, *20*, 5167–5173.
[107] L. Chen, Y. Li, S.-P. Li, L.-Z. Fan, C.-W. Nan, J. B. Goodenough, *Nano Energy* **2018**, *46*, 176–184.
[108] Y. Kim, I. Waluyo, A. Hunt, B. Yildiz, *Adv. Energy Mater.* **2022**, *12*, 2102741.
[109] Y. Arinicheva, X. Guo, M.-T. Gerhards, F. Tietz, D. Fattakhova-Rohlfing, M. Finsterbusch, A. Navrotsky, O. Guillon, *Chem. Mater.* **2022**, *34*, 1473–1480.
[110] B. Wang, G. Wang, P. He, L.-Z. Fan, *J. Membr. Sci.* **2022**, *642*, 119952.
[111] H. Huo, J. Liang, N. Zhao, X. Li, X. Lin, Y. Zhao, K. Adair, R. Li, X. Guo, X. Sun, *ACS Energy Lett.* **2020**, *5*, 2156–2164.
[112] L. Chen, X. Qiu, Z. Bai, L.-Z. Fan, *J. Energy Chem.* **2021**, *52*, 210–217.
[113] F. Aguesse, V. Roddatis, J. Roqueta, P. García, D. Pergolesi, J. Santiso, J. A. Kilner, *Solid State Ionics* **2015**, *272*, 1–8.
[114] C. Liu, H.-R. Wang, T. Long, Q. Ma, P. Ning, X.-R. Dong, C.-S. Zhou, X.-W. Wu, X.-X. Zeng, *ACS Appl. Energ. Mater.* **2022**, *5*, 3734–3740.
[115] G. Wang, H. Liu, Y. Liang, C. Wang, L.-Z. Fan, *Energy Storage Mater.* **2022**, *45*, 1212–1219.
[116] W. Li, X. Zhu, N. Zhou, Y. Yang, R. Li, C. Wang, Z. Fang, X. Ma, W. Zhao, X. Fu, W. Yan, *ACS Appl. Energ. Mater.* **2021**, *4*, 4772–4785.
[117] C. Wang, J. Liang, J. Luo, J. Liu, X. Li, F. Zhao, R. Li, H. Huang, S. Zhao, L. Zhang, J. Wang, X. Sun, *Sci. Adv.* **2021**, *7*, eabh1896.
[118] W.-H. Huang, X.-M. Li, X.-F. Yang, X.-X. Zhang, H.-H. Wang, H. Wang, *Mater. Chem. Front.* **2021**, *5*, 3593–3613.
[119] R. Zhao, Y. Wu, Z. Liang, L. Gao, W. Xia, Y. Zhao, R. Zou, *Energy Environ. Sci.* **2020**, *13*, 2386–2403.
[120] R. Hou, M. Miao, Q. Wang, T. Yue, H. Liu, H. S. Park, K. Qi, B. Y. Xia, *Adv. Energy Mater.* **2020**, *10*, 1901892.
[121] Y. Yoshida, K. Fujie, D. Lim, R. Ikeda, H. Kitagawa, *Angew. Chem. Int. Ed.* **2019**, *58*, 10909–10913; *Angew. Chem.* **2019**, *131*, 11025–11029.
[122] W. Gu, F. Li, T. Liu, S. Gong, Q. Gao, J. Li, Z. Fang, *Adv. Sci.* **2022**, *9*, 2103623.
[123] C. Niu, W. Luo, C. Dai, C. Yu, Y. Xu, *Angew. Chem. Int. Ed.* **2021**, *60*, 24915–24923; *Angew. Chem.* **2021**, *133*, 25119–25127.
[124] S. H.-S. Cheng, K.-Q. He, Y. Liu, J.-W. Zha, M. Kamruzzaman, R. L.-W. Ma, Z.-M. Dang, R. K. Y. Li, C. Y. Chung, *Electrochim. Acta* **2017**, *253*, 430–438.
[125] J. Feng, L. Wang, Y. Chen, P. Wang, H. Zhang, X. He, *Nano Convergence* **2021**, *8*, 2.
[126] R. Chen, W. Qu, X. Guo, L. Li, F. Wu, *Mater. Horiz.* **2016**, *3*, 487–516.
[127] Z. Xu, T. Yang, X. Chu, H. Su, Z. Wang, N. Chen, B. Gu, H. Zhang, W. Deng, H. Zhang, W. Yang, *ACS Appl. Mater. Interfaces* **2020**, *12*, 10341–10349.
[128] L. Xu, *Mater. Chem. Front.* **2021**, *5*, 1315–1323.
[129] L. Wang, Y. Zhong, Z. Wen, C. Li, J. Zhao, M. Ge, P. Zhou, Y. Zhang, Y. Tang, G. Hong, *Sci. China Mater.* **2022**, *65*, 2179–2188.
[130] B. M. Savoie, M. A. Webb, T. F. Miller III, *J. Phys. Chem. Lett.* **2016**, *8*, 641–646.
[131] D. Li, J. Wang, S. Guo, Y. Xiao, Q. Zeng, W. He, L. Gan, Q. Zhang, S. Huang, *Adv. Funct. Mater.* **2020**, *30*, 2003945.
[132] Z. Zeng, G. Liu, Z. Jiang, L. Peng, J. Xie, *J. Power Sources* **2020**, *451*, 227730.
[133] T. Famprikis, P. Canepa, J. A. Dawson, M. S. Islam, C. Masquelier, *Nat. Mater.* **2019**, *18*, 1278–1291.
[134] S. Hu, L. Du, G. Zhang, W. Zou, Z. Zhu, L. Xu, L. Mai, *ACS Appl. Mater. Interfaces* **2021**, *13*, 13183–13190.
[135] T. Wu, W. Dai, M. Ke, Q. Huang, L. Lu, *Adv. Sci.* **2021**, *8*, 2100774.
[136] W. Liu, D. Lin, J. Sun, G. Zhou, Y. Cui, *ACS Nano* **2016**, *10*, 11407–11413.
[137] H. Chen, D. Adekoya, L. Hencz, J. Ma, S. Chen, C. Yan, H. Zhao, G. Cui, S. Zhang, *Adv. Energy Mater.* **2020**, *10*, 2000049.
[138] M. Jia, Z. Bi, C. Shi, N. Zhao, X. Guo, *J. Power Sources* **2021**, *486*, 229363.
[139] K. He, C. Chen, R. Fan, C. Liu, C. Liao, Y. Xu, J. Tang, R. K. Y. Li, *Compos. Sci. Technol.* **2019**, *175*, 28–34.
[140] G. D. Salian, C. Lebouin, A. Galeyeva, A. P. Kurbatov, T. Djenizian, *Front. Chem.* **2019**, *6*, 675.
[141] J. B. Goodenough, *J. Solid State Electrochem.* **2012**, *16*, 2019–2029.
[142] C. Wang, H. Liu, Y. Liang, D. Li, X. Zhao, J. Chen, W. Huang, L. Gao, L.-Z. Fan, *Adv. Funct. Mater.* **2022**, *33*, 2209828.
[143] W. Liang, Y. Shao, Y.-M. Chen, Y. Zhu, *ACS Appl. Energ. Mater.* **2018**, *1*, 6064–6071.
[144] Z. Fang, Y. Luo, H. Liu, Z. Hong, H. Wu, F. Zhao, P. Liu, Q. Li, S. Fan, W. Duan, J. Wang, *Adv. Sci.* **2021**, *8*, 2100736.
[145] F. He, W. Tang, X. Zhang, L. Deng, J. Luo, *Adv. Mater.* **2021**, *33*, 2105329.
[146] Z. Xie, Z. Wu, X. An, X. Yue, P. Xiaokaiti, A. Yoshida, A. Abudula, G. Guan, *J. Membr. Sci.* **2020**, *596*, 117739.
[147] L. Lin, K. Qin, M. Li, Y. Hu, H. Li, X. Huang, L. Chen, L. Suo, *Energy Storage Mater.* **2022**, *45*, 821–827.
[148] Y. Li, G. Wang, L.-Z. Fan, *Batteries & Supercaps* **2022**, *5*, e202200212.
[149] P. P. Paul, *Energy Storage Mater.* **2022**, *45*, 969–1001.
[150] T.-S. Wang, X. Liu, Y. Wang, L.-Z. Fan, *Adv. Funct. Mater.* **2021**, *31*, 2001973.
[151] L. Chen, W. Li, L. Fan, C. Nan, Q. Zhang, *Adv. Funct. Mater.* **2019**, *29*, 1901047.
[152] S. Xiong, Y. Liu, P. Jankowski, Q. Liu, F. Nitze, K. Xie, J. Song, A. Matic, *Adv. Funct. Mater.* **2020**, *30*, 2001444.
[153] Y. Liang, H. Liu, G. Wang, C. Wang, Y. Ni, C. Nan, L. Fan, *InfoMat* **2022**, *4*, e12292.
[154] W. Choi, S. Park, W. Jung, D. H. Won, J. Na, Y. J. Hwang, *ACS Energy Lett.* **2022**, *7*, 939–945.
[155] X. Ma, L. Azhari, Y. Wang, *Chem* **2021**, *7*, 2843–2847.
[156] B. Jiang, W. E. Gent, F. Mohr, S. Das, M. D. Berliner, M. Forsuelo, H. Zhao, P. M. Attia, A. Grover, P. K. Herring, M. Z. Bazant, S. J. Harris, S. Ermon, W. C. Chueh, R. D. Braatz, *Joule* **2021**, *5*, 3187–3203.
[157] S. Müller, C. Sauter, R. Shunmugasundaram, N. Wenzler, V. De Andrade, F. De Carlo, E. Konukoglu, V. Wood, *Nat. Commun.* **2021**, *12*, 6205.
[158] F. Liu, R. Xu, Y. Wu, D. T. Boyle, A. Yang, J. Xu, Y. Zhu, Y. Ye, Z. Yu, Z. Zhang, X. Xiao, W. Huang, H. Wang, H. Chen, Y. Cui, *Nature* **2021**, *600*, 659–663.
[159] X.-X. Wang, X.-W. Chi, M.-L. Li, D.-H. Guan, C.-L. Miao, J.-J. Xu, *Chem* **2022**, *9*, 390-410.
[160] Q. Wang, G. Zhang, Y. Li, Z. Hong, D. Wang, S. Shi, *Npj Comput. Mater.* **2020**, *6*, 1–8.

Manuscript received: November 18, 2022
Revised manuscript received: December 24, 2022
Version of record online: February 10, 2023